AWARD NUMBER: W81XWH-14-1-0525

TITLE: Overcoming Drug-Resistant Prostate Cancer with APE1/Ref-1 Blockade

PRINCIPAL INVESTIGATOR: Travis Jerde

CONTRACTING ORGANIZATION: Indiana University, Indianapolis
Indianapolis, IN 46202-5126

REPORT DATE: October 2016

TYPE OF REPORT: Annual

PREPARED FOR: U.S. Army Medical Research and Materiel Command
Fort Detrick, Maryland 21702-5012

| 1. REPORT DATE | 2. REPORT TYPE | 3. DATES COVERED |
|---|---|---|
| October 2016 | Annual | 09/30/2015 – 09/29/2016 |

**4. TITLE AND SUBTITLE**
Overcoming Drug-Resistant Prostate Cancer with APE1/Ref-1 Blockade

**5a. CONTRACT NUMBER**
W81XWH-14-1-0525

**5b. GRANT NUMBER**

**5c. PROGRAM ELEMENT NUMBER**

**6. AUTHOR(S)**

Travis J. Jerde, PhD

E-Mail: tjjerde@iupui.edu

**5d. PROJECT NUMBER**
0010494783-0001

**5e. TASK NUMBER**

**5f. WORK UNIT NUMBER**

**7. PERFORMING ORGANIZATION NAME(S) AND ADDRESS(ES)**

Indiana University, Indiana
Office of Research Administration
980 Indiana Avenue
Lockefield 2232
Indianapolis, IN 46202-2915

**8. PERFORMING ORGANIZATION REPORT NUMBER**

**9. SPONSORING / MONITORING AGENCY NAME(S) AND ADDRESS(ES)**

U.S. Army Medical Research and Materiel Command
Fort Detrick, Maryland 21702-5012

**10. SPONSOR/MONITOR'S ACRONYM(S)**

**11. SPONSOR/MONITOR'S REPORT NUMBER(S)**

**12. DISTRIBUTION / AVAILABILITY STATEMENT**

Approved for Public Release; Distribution Unlimited

**13. SUPPLEMENTARY NOTES**

**14. ABSTRACT**

We have identified a new target that might explain how advanced prostate cancer cells avoid being killed by chemotherapy: Apurinic/apyrimidinic endonuclease/redox-factor 1, or simply, Ref-1, for short. In this report, we provide evidence that APE1/Ref-1 is induced in prostate cancer cells and in human prostate cancer. This expression correlates to inflammation and to survivin signaling in human prostate cancer specimens. Genetic knockdown of APE1/Ref-1 disrupts prostate cancer cell growth and survival in cell culture. In addition, inhibition of the redox function selectively of Ref-1 results in cell growth inhibition, with this therapy preferentially inhibiting prostate cancer cell growth above that in non-cancerous cells. Specific blockade of Ref-1 redox activity in tumors is a novel concept in tumor therapy. If we are successful, we will have defined a critical therapeutic target for drug-resistant prostate cancers, and logically clinical trials would follow targeting this pathway.

**15. SUBJECT TERMS**
Nothing listed

| 16. SECURITY CLASSIFICATION OF: | | | 17. LIMITATION OF ABSTRACT | 18. NUMBER OF PAGES | 19a. NAME OF RESPONSIBLE PERSON |
|---|---|---|---|---|---|
| a. REPORT | b. ABSTRACT | c. THIS PAGE | | | USAMRMC |
| U | U | U | UU | 54 | 19b. TELEPHONE NUMBER *(include area code)* |

## Table of Contents

## 1. INTRODUCTION:

We hypothesize that Human apurinic/apyrimidinic endonuclease/redox-factor 1 (APE1/Ref-1, or Ref-1) enhances transcriptional activator activity thereby inducing expression of the survival protein survivin during drug resistance. In Aim 1 of this work, we have proposed to determine Ref-1's role in prostate cancer cells and evaluate the mechanisms by which it exerts its effect. In Aim 2 of the funded proposal, we have proposed to determine if STAT3 inhibition results in activation of compensatory pathways of survival protein induction, and if Ref-1 activates AP-1 in response to STAT3 inhibition, specifically in taxane-resistant cells. In Aim 3 of the proposal, we he proposed determine if Ref-1 mediates taxane-resistance in prostate cancer cells and if pharmacological inhibition of Ref-1 with novel but tested inhibitors renders drug-resistant cells sensitive to taxanes, both in vitro and in vivo. The proposal integrates human prostate tissue specimens including drug-resistant metastases with cell culture and *in vivo* animal models. This work may therefore provide the mechanistic basis for a novel combination therapy trial in chemo-resistant prostate cancer, and may therefore be the genesis of a therapeutic for prostate cancer patients.

## 2. KEYWORDS:

Prostate cancer, taxane resistance, Human apurinic/apyrimidinic endonuclease/redox-factor 1 (APE1/Ref-1), survivin

## 3. OVERALL PROJECT SUMMARY:

Summarize the progress during appropriate reporting period (single annual or comprehensive final). This section of the report shall be in direct alignment with respect to each task outlined in the approved SOW in a summary of Current Objectives, and a summary of Results, Progress and Accomplishments with Discussion. Key methodology used during the reporting period, including a description of any changes to originally proposed methods, shall be summarized. Data supporting research conclusions, in the form of figures and/or tables, shall be embedded in the text, appended, or referenced to appended manuscripts. Actual or anticipated problems or delays and actions or plans to resolve them shall be included. Additionally, any changes in approach and reasons for these changes shall be reported. **Any change that is substantially different from the original approved SOW (e.g., new or modified tasks, objectives, experiments, etc.) requires review by the Grants Officer's Representative and final approval by USAMRAA Grants Officer through an award modification prior to initiating any changes.**

The following is a timeline for tasks, year by year, in the approved statement of work:
Previously completed (year one) tasks are in red font. The tasks to be completed **in year two** are highlighted in yellow, and bolded.

| **Specific Aim 1 :To determine the impact of Ref-1 mediated STAT3 activity on survival pathway activation in prostate cancer cell lines and human cancer tissues.** | **Timeline (Months)** | **Site 1 PI: Jerde** |
|---|---|---|
| **Major Task 1:** ***Ref-1 co-localization with STAT3 and survival signaling in human prostate cancer:*** | 1-12 | |
| **Subtask1: IRB in hand; acquire specimens** | **1-3** | Drs. Jerde/ Chang |
| **Subtask 2: Stain and correlation of human specimens** | **1-6** | Dr. Jerde |
| **Subtask 3: Correlation of staining and quantification** | **6-7** | Dr. Jerde |
| **Milestone(s) Achieved: determining co-localization; writing and publishing manuscript** | ***7-12*** | |
| **Local IRB/IACUC Approval** | **1** | |
| **Milestone Achieved: HRPO/ACURO Approval** | **1** | |
| **Major Task 2:** ***Effect of Ref-1 on STAT3 activity and survival signaling*** | | |
| **Subtask 1: Ref-1 siRNA** | **1-3** | Drs. Jerde/ Fishel |
| **Subtask 2: Overexpression of wt-Ref-1** | **3-6** | Drs. Jerde/ Fishel |
| **Subtask 3: Mutant Ref-1 constructs (C65A)** | **4-8** | Drs. Jerde/ Fishel |
| **Subtask 4: selective Ref-1 redox inhibitor, E3330** | **6-10** | Drs. Jerde/ Fishel |
| **Milestone(s) Achieved: Determining that Ref-1 regulates STAT3-initiated transcription of target genes, that STAT3 activity and survival will be dependent upon intact Ref-1, functioning through its redox function. Manuscript** | ***7-12*** | |
| **Specific Aim 2 : To determine if Ref-1 inhibition circumvents transcriptional functional compensation triggered by STAT3 inhibitors.** | **Timeline (Months)** | **Site 1 PI: Jerde** |
| **Major Task 3:** ***Compensatory response in drug resistant and sensitive cell lines-establishing the compensatory response*** | 6-15 | |
| Subtask1: Constructs of STAT3 and AP-1 promoters driving GFP-Luc gene reporters | **6-8** | Drs. Jerde/ Fishel |
| Subtask 2: Assess cell lines with STATTIC | 8-12 | Drs. Jerde/ Fishel |
| Subtask 3: Assess pathway activation for each transcription activator | 12-15 | Drs. Jerde/ Fishel |
| Milestone(s) Achieved: Characterization of the STAT3 inhibition compensatory response | *15* | |
| **Major Task 4*: Assessing Ref-1's role in compensatory signaling*** | 6-24 | |
| **Subtask 1: Constructs of STAT3 and AP-1 promoters driving GFP-Luc gene reporters** | **6-8** | Drs. Jerde/ Fishel |
| Subtask 2: Treatment with E3330, STATTIC, | 15-21 | Drs. Jerde/ Fishel/ Kelley |
| Subtask 3: Mutant Ref-1 constructs (C65A) | 21-24 | Drs. Jerde/ Fishel |
| Milestone(s) Achieved: Determining role of STAT3 compensatory response on Ref-1 function in docetaxel-resistant lines-quantified data | 24 | |
| **Major Task 5:** ***Assessing Ref-1 driven compensatory signaling in graft tumors*** | 12-30 | |
| Subtask 1: Grow graft tumors and treat animals with STAT3 inhibitors-assess outcome by luminescence and gene expression. | 12-24 | Drs. Jerde/ Ratliff/ Kelley |

| | | |
|---|---|---|
| 2 cell lines x 3 constructs x 2 treatments x8 per group x 3 sacrifice times=288 mice. 21 day tumor growth, plus 3 day analysis, plus 7 day acclimation time=31 days house per mouse | | |
| Milestone(s) Achieved: Determining in vivo STAT3 compensatory response.<br>Publish manuscript | 24-30 | |
| **Specific Aim 3: To determine if Ref-1 inhibition sensitizes drug resistance in prostate cancers to chemotherapy.** | | **Site 1<br>PI: Jerde** |
| **Major Task 6:** ***Evaluating Ref-1 expression in drug-resistant human prostate cancer metastases*** | 1-30 | |
| **Subtask1: Acquire specimens** | **1-24** | Drs. Jerde/ Chang |
| **Subtask 2: Stain and correlation of human specimens** | **1-25** | Dr. Jerde |
| Subtask 3: Correlation of staining and quantification | 25-26 | Dr. Jerde |
| Milestone(s) Achieved: determining co-localization; writing and publishing manuscript | *26-30* | |
| **Major Task 7*: Determining the effect of Ref-1 on docetaxel-resistant prostate cancer*** | 12-21 | |
| Subtask 1: Transfect docetaxel-resistant C4-2 ($C4\text{-}2^{doc}$) and PC3 cells ($PC3^{doc}$) with siRNA | 12-15 | Drs. Jerde/ Fishel |
| Subtask 2: CRC in transfected cells, with or without inhibitors | 15-18 | Drs. Jerde/ Fishel |
| Subtask 3: Mutant Ref-1 constructs (C65A) | 19-21 | Drs. Jerde/ Fishel |
| Milestone(s) Achieved: Determining Ref-1 function in docetaxel-resistant lines-quantified data | 12-21 | |
| **Major Task 8:** ***Effect of Ref-1 inhibition on in vivo models of prostate cancer*** | 18-36 | |
| Subtask 1: Docetaxel-resistant and parental C4-2 and PC3 cells in vivo by subcutaneous implant<br>4 cell lines x 4 treatments x 8 per group =128 mice. 21 day tumor growth, plus 12 day analysis, plus 7 day acclimation time=40 days house per mouse | 18-30 | Drs. Jerde/ Ratliff |
| Subtask 2: Molecular analysis of tumor graft. | 28-36 | Drs. Jerde/ Ratliff |
| Milestone(s) Achieved: demonstrate Ref-1 inhibition in vivo blocks tumor growth and metastasis | 24-30 | |
| Milestone(s) Achieved: Publish manuscript demonstrating this effect.<br>Begin to acquire clinical trial documents for future study in humans | 30-36 | Drs. Jerde/ Kelley |

**Summary, year two tasks:**

**Specific Aim 1 :To determine the impact of Ref-1 mediated STAT3 activity on survival pathway activation in prostate cancer cell lines and human cancer tissues.**

**Milestone:** We have submitted a second manuscript from this proposal (referenced in the publication section, below) that demonstrates that APE1/Ref-1 is induced in prostate cancer cells and his highly expressed in human cancer, and it co-expresses with survivin and other survival proteins. Inhibition of APE1/Ref-1 with selective redox inhibitors halts prostate cancer cell growth and induced apoptosis. This manuscript is under review at *Oncotarget*, manuscript attached.

**Specific Aim 2 : To determine if Ref-1 inhibition circumvents transcriptional functional compensation triggered by STAT3 inhibitors.**

**Major Task 3:** ***Compensatory response in drug resistant and sensitive cell lines-establishing the compensatory response***
and
**Major Task 4*****: Assessing Ref-1's role in compensatory signaling***

Our first experiments showed some activities of STAT3 inhibitors in prostate cancer cells, and that APE1/Ref-1 inhibition did circumvent STAT3 inhibitor failures in taxane-resistant cells (Figure 1). In these experiments, we transfected parental PC3 cells ($PC3^{par}$) and docetaxel-resistant PC3 cells ($PC3^{doc}$) cells with siRNA to Ref-1 or scrambled control and treated them with docetaxel (30 ng/ml) or vehicle to determine if Ref-1 blockade sensitizes resistant cells to docetaxel. Docetaxel killed nearly all $PC3^{par}$ cells, and reduced the number of viable $PC3^{doc}$ cells per field by 65% in Ref-1-inhibited cells but had no effect in cells transfected with scrambled siRNA. **(Figure 1A)** We also determined if selective Ref-1 redox function inhibition with E3330 affected downstream Ref-1 effectors STAT3 and survivin. Inhibition of all three proteins similarly reduced cell number in parental cells. While Ref-1 inhibition sensitized $PC3^{doc}$ cells to docetaxel, survivin inhibition (YM-155 and LZQ-7F) only partially sensitized these cells to docetaxel, but STAT3 inhibition (STATTIC) failed to inhibit growth in these cells or sensitize them to docetaxel. **(Figure 1B)** These data partially support our original hypothesis that redox function of Ref-1 specifically participates in the development of docetaxel-resistance in prostate cancer cells, and they suggest that compensatory mechanisms to STAT3 inhibition are induced during the process of docetaxel resistance in these cells.

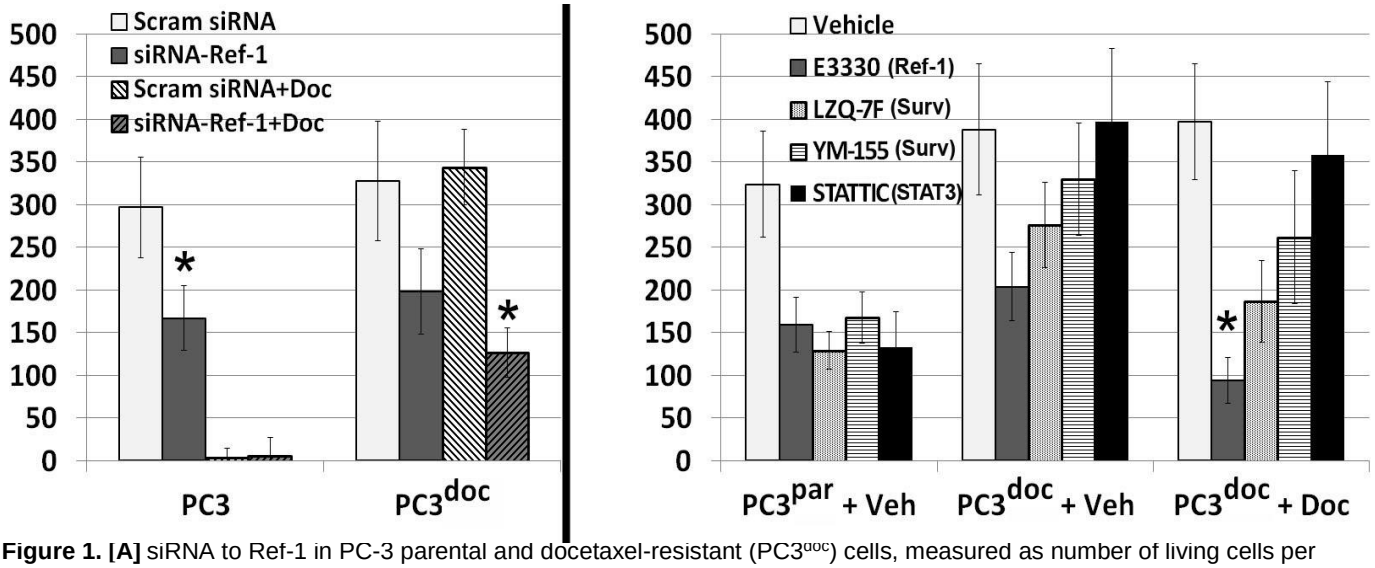


**Figure 1. [A]** siRNA to Ref-1 in PC-3 parental and docetaxel-resistant ($PC3^{doc}$) cells, measured as number of living cells per 20x field after 48 hours of treatment (n=3; * $p<0.05$—siRNA Ref-1 vs scrambled). siRNA knockdown was verified by 70% reduction in expression by quantified immunoblot (not shown); docetaxel concentration was 30 ng/ml. **[B]** Parental and Docetaxel-resistant $PC3^{doc}$ cells were tested with the previously-determined $EC_{50}$ concentrations of inhibitors of Ref-1 (E3330), survivin (LZQ-7F and YM-155), and STAT3 (STATTIC) and measured as number of living cells per 20x field after 48 hours of treatment (n=4; * $p<0.05$—drug+docetaxel versus drug alone).

Despite this, our further investigation into other signaling pathways that may be involved in Ref-1 function showed that the primary role that the APE1/Ref-1 played in our cells was through the transcription factor NFκB, not STAT3. **(Detailed in Figure 2)** Here, C4-2 cells were treated with DMSO or APX2009 (14 μM) for 12 hours. RNA was collected and RT-qPCR was performed using a primer/probe set for survivin (BIRC5) and HPRT1 for the internal control gene **(Figure 2A).** Survivin mRNA was significantly reduced upon treatment with the RQ value being <0.5. Because it has been shown in other cancers that survivin is a gene target of NFκB and that NFκB is regulated by APE1/Ref-1, we evaluated the ability of these two proteins to physically interact with each other and the cellular localization of both NFκB and APE1 upon treatment with APX2009. In **Figure 2B**, we demonstrate via co-immunoprecipitation that APE1/Ref-1 interacts with NFκB subunit p65 when using an APE1/Ref-1

antibody and in reverse experiments using a p65 antibody. In **Figure 2C**, p65 and APE1/Ref-1 were found to be co-localized in the nucleus but p65 nuclear localization was diminished upon treatment with APX2009 suggesting disturbed NFκB signaling. To determine if NFκB signaling is regulated by APE1/Ref-1 redox activity, we transfected C4-2 cells with NFκB-driven luciferase constructs. Treatment of these cells with APX2009 results in a significant decrease, in both basal NFκB activity and TNFa-induced activity **(Figure 2D)**. Because of this, we are now investigating this transcription factor, and its inhibitors for therapeutic use in this project.

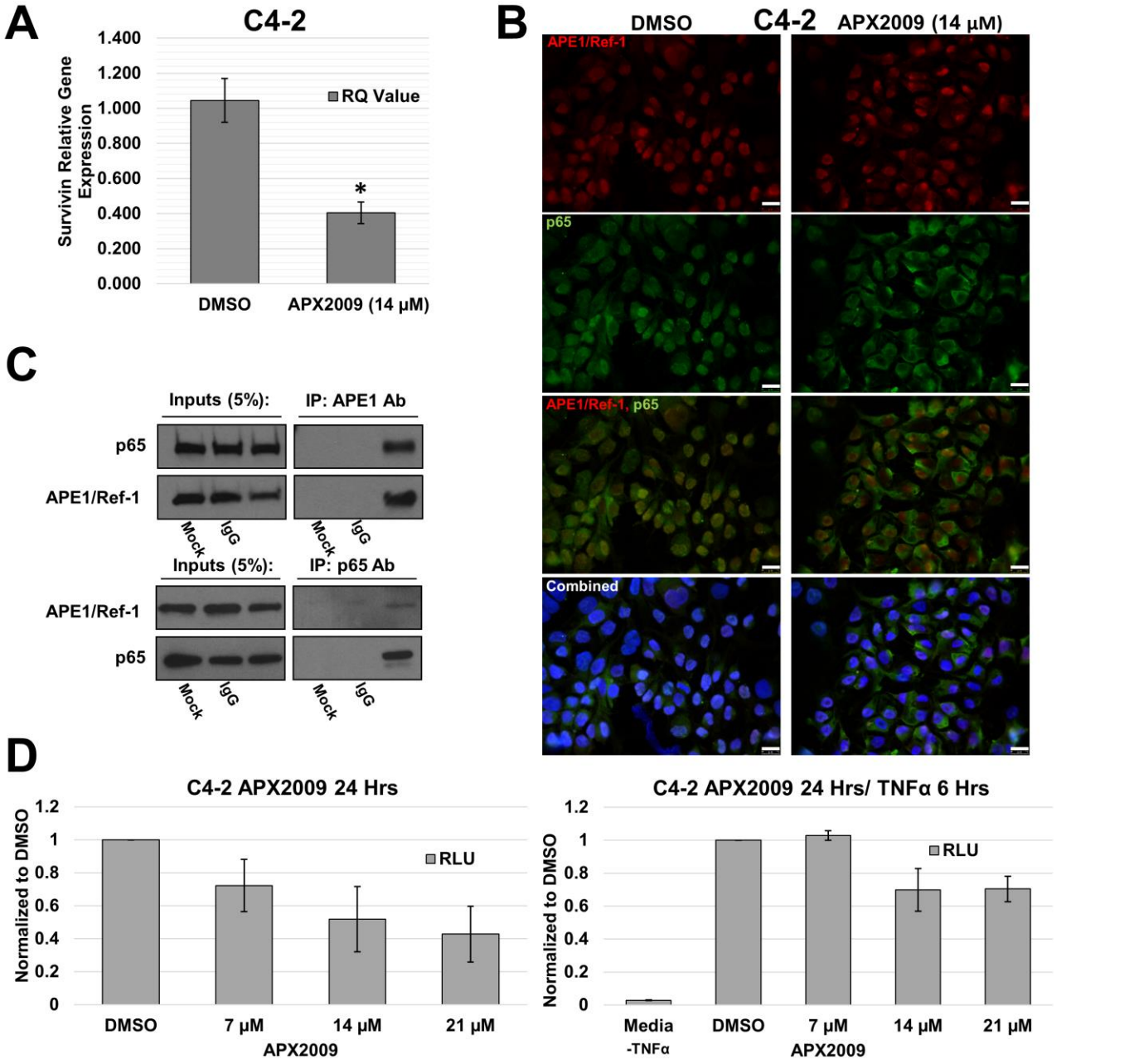


**Figure 2.** APE1/Ref-1 redox inhibition decreases survivin protein levels via NFκB. **A:** C4-2 cell line was treated with DMSO or APX2009 (14 μM) for 12 hours. RNA was isolated and RT-PCR for survivin was performed with HPRT1 as the internal control. **B:** C4-2 cell line was treated with DMSO or APX2009 for 48 Hrs and immunofluorescence was perfumed using antibodies for APE1/Ref-1 (Red) and NFκB subunit p65 (Green). Representative images were taken. Scale bar = 50 μM. **C:** Western blot validation of APE1/Ref-1 and p65 Co-Immunoprecipitation (CoIP) reactions. The input and IP were loaded for each reaction. Mock beads and generic IgG were used as negative controls. **D:** C4-2 cells were transfected with NFκB–Luc construct and co-transfected with a Renilla vector, pRL-TK. After 16 hrs, cells were treated with APX2009 for 24 hrs, and Firefly and Renilla luciferase activities were assayed using Renilla luciferase activity for normalization. All transfection experiments were performed in triplicate and repeated 3 times in independent experiments. Data are expressed as Relative Luciferase Units (RLU) normalized to DMSO showing the mean ± SEM.

In addition, we have also fully defined and determined the role in cell cycle arrest, G1 phase, by flow cytometry. **(Figure 3)**. In these experiments, PC-3 and C4-2 cells were treated with either DMSO or APX2009 (9 µM and 14 µM, respectively) for 48 hrs **(Figure 3A)** and cell lysates were collected for immunoblotting **(Figure 3B)**. After APX2009 treatment, both PC-3 and C4-2 cells displayed an altered, flattened cellular morphology. However, treatment with these compounds did not induce cell death as determined by both a lack of increased caspase 3 cleavage and a lack of increase in TUNEL labeling. Because no increase in apoptosis was detected and G2/M cell cycle proteins were decreased, cell cycle analysis was performed with Propidium Iodide (PI) staining. PC-3 and C4-2 cells were treated with APX2009 (9 µM and 14 µM, respectively) for 48 hrs and then stained with PI and analyzed by flow cytometry. **(Figure 3 C, D)** We found that the percentage of cells in G1 significantly increased, $p<0.05$ via Student's t-test, from 58 to 68% and 63 to 74% in PC3 and C4-2 cells, respectively. These effects on the cell cycle progression are similar to other recent reports of APE1/Ref-1 redox inhibition in cancer.

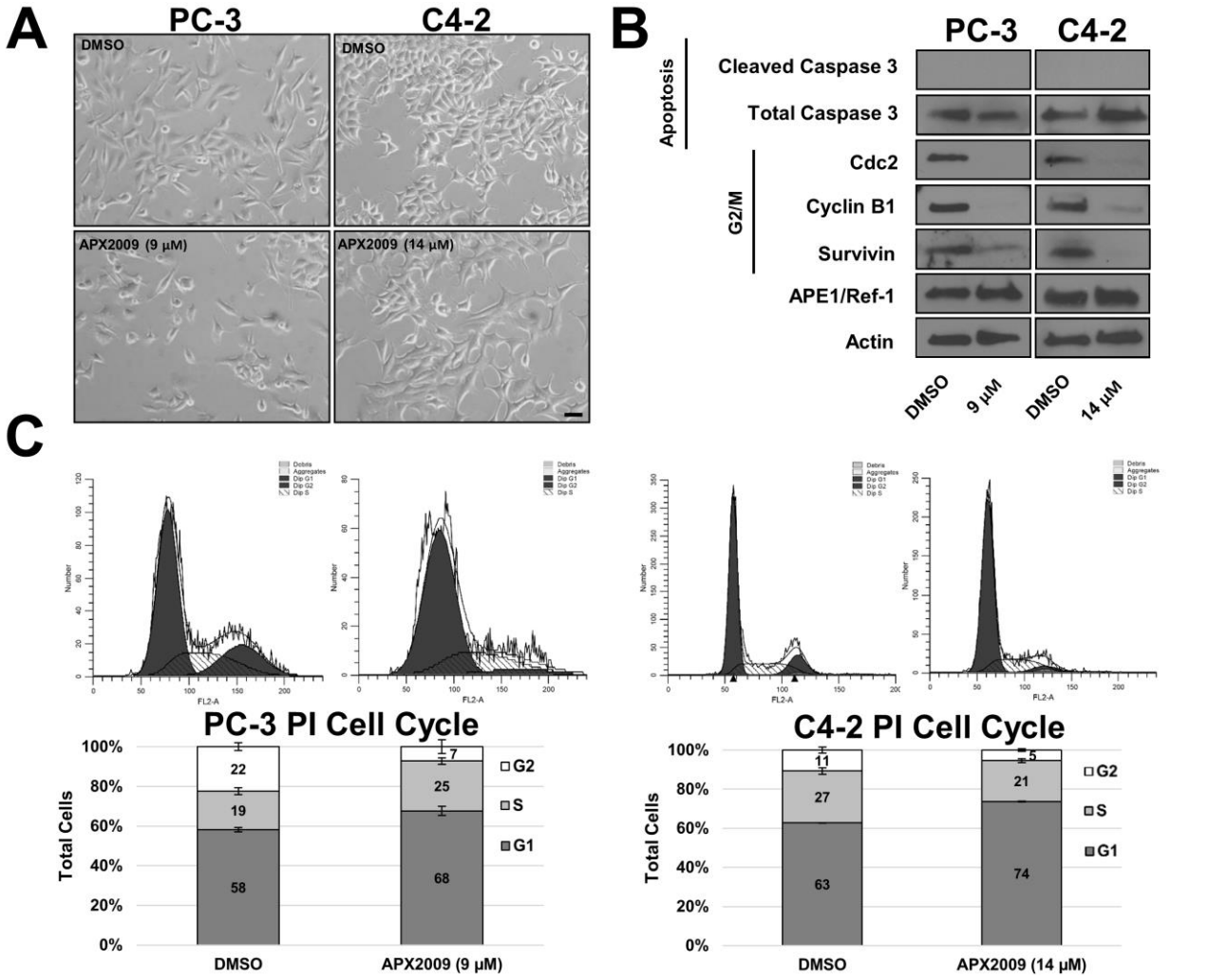


**Figure 3** APE1/Ref-1 redox inhibition induces $G_1$ cell arrest. **A:** PC-3 and C4-2 cell lines were treated with DMSO or APX2009 (9 and 14 µM, respectively) for 48 hours. Representative images were taken at 20X Magnification. Scale bar = 50 µm. **B:** Immunoblotting was performed and membranes were probed with antibodies for Cleaved Caspase 3, Total Caspase, Cyclin B1, Cdc2, survivin and Actin as labeled**. C,D:** PC-3 and C4-2 cells were treated with DMSO or APX2009 (9 and 14 µM, respectively) for 48 hrs and then collected and stained with RNAse/PI wash. Flow Cytometry was then performed (N=3).

**Major Task 6:** ***Evaluating Ref-1 expression in <u>drug-resistant</u> human prostate cancer metastases***

We are currently finishing our staining of our 14 prostate cancer metastasis. This will be published in 2017.

**Major Task 7*: Determining the effect of Ref-1 on docetaxel-resistant prostate cancer***

We have completed generating all cell lines described in the Statement of Work, and are investigating these questions outlined in tasks 7 and 8.

4. **KEY RESEARCH ACCOMPLISHMENTS:** Bulleted list of key research accomplishments emanating from this research. Project milestones, such as simply completing proposed experiments, are not acceptable as key research accomplishments. Key research accomplishments are those that have contributed to the major goals and objectives and that have potential impact on the research field.

   1. Identified that APE1/Ref-1 is highly expressed in human prostate cancers.
   2. Discovered that APE1/Ref-1 is correlated to survivin expression in human prostate cancers.
   3. Published manuscript showing that inflammation induces survivin expression in experimental models and that it correlates to sites of inflammation in human prostate cancer. (Attached)
   4. Submitted a manuscript that found that redox-specific Ref-1 inhibition inhibits selectively prostate cancer cell growth above that of non-cancerous prostate cancer cells. (Attached)
   5. Discovered that APE1/Ref-1 redox inhibition induces G1 cell arrest.
   6. Discovered that APE1/Ref-1 redox inhibition decreases survivin protein levels via NFκB and that this transcription factor, more than STAT3, is responsible for APE1/Ref-1 mediated effects in prostate cancer cells.

5. **CONCLUSION:** Summarize the importance and/or implications with respect to medical and /or military significance of the completed research including distinctive contributions, innovations, or changes in practice or behavior that has come about as a result of the project. A brief description of future plans to accomplish the goals and objectives shall also be included.

   We have found that the multi-functional protein APE1/Ref-1 is induced in prostate cancer cells and in human prostate cancer. This expression correlates to inflammation and to survivin signaling in human prostate cancer specimens. Genetic knockdown of APE1/Ref-1 disrupts prostate cancer cell growth and survival in cell culture. In addition, inhibition of the redox function selectively of Ref-1 results in cell growth inhibition, with this therapy preferentially inhibiting prostate cancer cell growth above that in non-cancerous cells. Originally, this plan proposed that STAT3-mediated transcription factor activity was the mechanism by which APE1/Ref-1 exerted its effects, however our recent data show that the factor NFκB is more prominent in this role.

   In the coming year, we will complete the experiments outlined in major tasks 6, 7, and 8 of our statement of work. Inhibition of Ref-1 via siRNA and E3330 treatment restores taxane sensitivity in PCdoc cells, and we will determine if taxane-resistant metastases exhibit greater Ref-1 induction and activity than their sensitive counterparts and that drug-resistant prostate cancer cells become sensitive to docetaxel when challenged Ref-1 inhibition. Further, in vivo models will be utilized to test the effect of Ref-1 inhibition on tumor growth and progression, support targeting this pathway therapeutically in men with chemotherapy-resistant prostate cancer.

6. **PUBLICATIONS, ABSTRACTS, AND PRESENTATIONS:**

   a. List all manuscripts submitted for publication during the period covered by this report resulting from this project. Include those in the categories of lay press, peer-reviewed scientific journals, invited articles, and abstracts. Each entry shall include the author(s), article title, journal name, book title, editors(s), publisher, volume number, page number(s), date, DOI, PMID, and/or ISBN.

      **(1)** Lay Press: Nothing to report
      **(2)** Peer-Reviewed Scientific Journals:

**McIlwain DM, Snider BM, Zoetemelk M, Myers JD, Edwards ME, Jerde TJ. Coordinated induction of cell survival signaling in the inflamed microenvironment of the prostate. *The Prostate*, 2015**

**McIlwain DW, Fishel ML, Kelley MR, Jerde TJ. APE1/Ref-1 regulates prostate cancer cell proliferation via survivin protein expression. *Oncotarget*, 2017.**

**(3)** Invited Articles: Nothing to report

**(4)** Abstracts: Nothing to report

b. List presentations made during the last year (international, national, local societies, military meetings, etc.). Use an asterisk (*) if presentation produced a manuscript.

**Plenary Invitation: Society of Basic Urological Research**
**Presented at the Annual Fall Meeting of the Society of Basic Urological Research, Ft. Lauderdale, FL, November 11, 2015**

7. **INVENTIONS, PATENTS AND LICENSES:** List all inventions made and patents and licenses applied for and/or issued. Each entry shall include the inventor(s), invention title, patent application number, filing date, patent number if issued, patent issued date, national, or international.

   **Nothing to report**

8. **REPORTABLE OUTCOMES:** Provide a list of reportable outcomes that have resulted from this research. Reportable outcomes are defined as a research result that is or relates to a product, scientific advance, or research tool that makes a meaningful contribution toward the understanding, prevention, diagnosis, prognosis, treatment and /or rehabilitation of a disease, injury or condition, or to improve the quality of life. This list may include development of prototypes, computer programs and/or software (such as databases and animal models, etc.) or similar products that may be commercialized.

   **As shown in key research findings, we have identified a mechanism by which prostate cancer cells survive the noxious conditions of the inflamed prostatic microenvironment.**

9. **OTHER ACHIEVEMENTS:** This list may include degrees obtained that are supported by this award, development of cell lines, tissue or serum repositories, funding applied for based on work supported by this award, and employment or research opportunities applied for and/or received based on experience/training supported by this award.

   **Nothing to report**

   For each section, 4 through 9, if there is no reportable outcome, state "Nothing to report."

10. **REFERENCES:** List all references pertinent to the report using a standard journal format (i.e., format used in *Science*, *Military Medicine*, etc.).

11. **APPENDICES:** Attach all appendices that contain information that supplements, clarifies or supports the text. Examples include original copies of journal articles, reprints of manuscripts and abstracts, a curriculum vitae, patent applications, study questionnaires, and surveys, etc.

**NOTE:**

**TRAINING OR FELLOWSHIP AWARDS:** For training or fellowship awards, in addition to the elements outlined above, include a brief description of opportunities for training and professional development. Training activities may include, for example, courses or one-on-one work with a mentor. Professional development activities may include workshops, conferences, seminars, and study groups.

**Not applicable**

**COLLABORATIVE AWARDS:** For collaborative awards, independent reports are required from BOTH the Initiating Principal Investigator (PI) and the Collaborating/Partnering PI. A duplicative report is acceptable; however, tasks shall be clearly marked with the responsible PI and research site. A report shall be submitted to **https://ers.amedd.army.mil** for each unique award.

**Not applicable**

**QUAD CHARTS:** If applicable, the Quad Chart (available on this eReceipt System https://cdmrp.org/Program_Announcements_and_Forms/ and under "Forms" on https://www.usamraa.army.mil) should be updated and submitted with attachments.

**Not applicable**

**MARKING OF PROPRIETARY INFORMATION:** Data that was developed partially or exclusively at private expense shall be marked as "Proprietary Data" and Distribution Statement B included on the cover page of the report. Federal government approval is required before including Distribution Statement B. The recipient/PI shall coordinate with the GOR to obtain approval. REPORTS NOT PROPERLY MARKED FOR LIMITATION WILL BE DISTRIBUTED AS APPROVED FOR PUBLIC RELEASE. It is the responsibility of the Principal Investigator to advise the GOR when restricted limitation assigned to a document can be downgraded to "Approved for Public Release." DO NOT USE THE WORD "CONFIDENTIAL" WHEN MARKING DOCUMENTS. See term entitled "Intangible Property – Data and Software Requirements" and https://mrmc.amedd.army.mil/index.cfm?pageid=researcher_resources.technical_reporting for additional information.

# Coordinated Induction of Cell Survival Signaling in the Inflamed Microenvironment of the Prostate

David W. McIlwain,[1] Marloes Zoetemelk,[2] Jason D. Myers,[1] Marshé T. Edwards,[3] Brandy M. Snider,[1] and Travis J. Jerde[1,4]*

[1]*Department of Pharmacology and Toxicology, Indiana University School of Medicine, Indianapolis, Indiana*
[2]*Inholland University, Hoofddorp, Netherlands*
[3]*Bennett College, Greensboro, North Carolina*
[4]*Melvin and Bren Simon Cancer Center-Indiana Basic Urological Research Working Group, Indiana University, Indianapolis, Indiana*

**PURPOSE.** Both prostate cancer and benign prostatic hyperplasia are associated with inflammatory microenvironments. Inflammation is damaging to tissues, but it is unclear how the inflammatory microenvironment protects specialized epithelial cells that function to proliferate and repair the tissue. The objective of this study is to characterize the cell death and cell survival response of the prostatic epithelium in response to inflammation.
**METHODS.** We assessed induction of cell death (TNF, TRAIL, TWEAK, FasL) and cell survival factors (IGFs, hedgehogs, IL−6, FGFs, and TGFs) in inflamed and control mouse prostates by ELISA. Cell death mechanisms were determined by immunoblotting and immunofluorescence for cleavage of caspases and TUNEL. Survival pathway activation was assessed by immunoblotting and immunofluorescence for Mcl−1, Bcl−2, Bcl−XL, and survivin. Autophagy was determined by immunoblotting and immunofluorescence for free and membrane associated light chain 3 (LC−3).
**RESULTS.** Cleavage of all four caspases was significantly increased during the first 2 days of inflammation, and survival protein expression was substantially increased subsequently, maximizing at 3 days. By 5 days of inflammation, 50% of prostatic epithelial cells expressed survivin. Autophagy was also evident during the recovery phase (3 days). Finally, immunofluorescent staining of *human* specimens indicates strong activation of survival proteins juxtaposed to inflammation in inflamed prostate specimens.
**CONCLUSIONS.** The prostate responds to deleterious inflammation with induction of cell survival mechanisms, most notably survivin and autophagy, demonstrating a coordinated induction of survival factors that protects and expands a specialized set of prostatic epithelial cells as part of the repair and recovery process during inflammation. *Prostate 76:722–734, 2016.* © 2016 Wiley Periodicals, Inc.

*KEY WORDS:* **prostate; inflammation; cell survival; cell death; repair**

## INTRODUCTION

Continual and recalcitrant inflammation is an extremely common condition in the human prostate and has been found to be associated with a number of prostatic diseases including prostate cancer and benign prostatic hyperplasia (BPH) [1–4]. Prostatic inflammation is characterized by the presence of inflammatory cells in the stroma, epithelium, and lumen of prostatic glands where the infiltrate is primarily lymphocytic with secondary accompanying macrophages juxtaposed

Grant sponsor: National Institutes of Health-NIDDK; Grant number: DK092366-01A1; Grant sponsor: Department of Pharmacology and Toxicology; Grant sponsor: Indiana University School of Medicine Melvin and Bren Simon Cancer Center; Grant sponsor: Indiana Clinical and Translational Sciences Institute (CTSI).

Conflicts of interest: none.

*Correspondence to: Travis J. Jerde, Ph.D., Assistant Professor of Pharmacology and Toxicology, A417 VanNuys Medical Sciences Building, 635 Barnhill Drive, Indianapolis, IN 46202.
E-mail: tjjerde@iupui.edu
Received 31 July 2015; Accepted 20 January 2016
DOI 10.1002/pros.23161
Published online 24 February 2016 in Wiley Online Library (wileyonlinelibrary.com).

to loci of reactive hyperplasia [1]. The origins of inflammation in the prostate remain a subject of debate and are most likely multi-factorial [5]. A role for a bacterial component in prostatic inflammation is controversial but is certainly plausible [6–9], and colonization by non-culturable organisms has been suggested by PCR assays of bacterial 16S ribosomal RNA in prostate biopsies as this has been associated with histological evidence of inflammation [10]. Numerous nonbacterial causes of inflammation have been investigated including viruses, environmental components, systemic hormones, and urinary reflux. Whatever the cause, inflammation in the prostate is of considerable importance to urological research due to the prevalence and impacts of BPH and prostate cancer.

While much has been described regarding prostate disease resulting from oxygen and nitrogen radicals during inflammation, proliferative mechanisms associated with repair and regeneration are less understood. Repair and regrowth are co-regulated processes characteristic of many cellular responses to trauma and in order for tissue recovery to proceed, inflammation must orchestrate precise series of events directing damaged cells to die, inducing proliferation of protected tissue progenitors to repopulate damaged tissue, and promoting differentiation of those expanded cells into proper cell subtypes [11]. Errors in these processes allow for expansion of damaged cells in an environment saturated in growth promoting factors leading to hyperplasia and desmoplasia [12]. While there is an extensive literature in prostate cancer cells regarding survival and cell death escape, mechanisms of how inflammation directs cells to avoid death and proliferate are poorly understood.

In addition to the classically understood mechanisms by which cells survive noxious tissue conditions—inhibition of pro-apoptotic proteins, induction of pro-survival proteins, and the subsequent inactivation of caspases—autophagy represents a process that can be associated with both the promotion of apoptosis and the promotion of cell survival and proliferation. Autophagy consists of autophagosome formation and effective macromolecule degradation [13]. The mechanisms of autophagy are diverse and depend on the origin of the stimulus. Autophagy is implicated in a number of diseases including cancer [14]. The removal of damaged organelles or proteins can be advantageous for a cell and may act as an escape mechanism from cell death [15].

It is not known how specialized cells in the prostatic epithelium are programmed to avoid cell death mechanisms in the noxious condition of inflammation and survive in order to repopulate the tissue as part of the innate repair and recovery process. In this study, we characterize the immediate induction of cell death mechanisms in our mouse model of prostatic inflammation that has been shown to transition from acute to chronic phases of inflammation similar to human prostates. Cell death signaling induction is followed by a coordinated induction of survival mechanisms that begin in basal epithelial cells and expand to include all layers of the epithelium. We also found that autophagy is induced during the recovery phases of inflammation. Finally, we found that the most consistently induced of the survival proteins, survivin, is associated with inflammation in human prostate specimens, and that survivin expression is more tightly correlated with inflammation than with disease state of the prostate.

## METHODS

### In Vivo Induction of Inflammation

All animal experiments were conducted under the approval and supervision of the Indiana University School of Medicine Animal Care and Use Committee, and in accordance of National Institutes of Health guidelines for animal research. *Escherichia coli* strain 1677 ($2 \times 10^6$/ml, 100 μl per mouse) was instilled through catheters into the urinary tract of C57BL/6J wild-type mice, as previously described [5,6,16]. Mice were then inoculated with 100 μl of BrdU (3.1 mg/ml Roche) for 2 hr before being sacrificed daily for 7 days after instillation, and their prostates were removed and separated by lobe (Ventral Prostate [VP], Coagulating Gland [CG], and Dorsolateral Prostate [DLP]) for molecular or histological analysis. PBS (Phosphate-buffered saline)-instilled animals were used as controls. Tissues were either paraffin-embedded for immunohistochemistical analysis or snap-frozen for molecular analysis. The *E. coli* strain 1667 in these experiments is being utilized as a tool for the induction of inflammation in the rodent prostate and has been shown to induce cellular effects that parallel that of inflammation found in a number of human prostatic diseases. In this model, the inflammatory response to bacterial inoculation is characterized by a primarily neutrophilic infiltrate in the first and second day that progresses to a primarily lymphocytic infiltrate 3–5 days post-inoculation. Macrophages are prevalent to a lesser degree throughout both acute and chronic stages. The chronic stage (days 3–5) has a very similar leukocytic content and distribution as that found in chronic human prostatic inflammation in benign or cancerous prostates [17,18]. The dorsolateral lobe of the rodent prostate has been demonstrated to produce the most dynamic and consistent resp onse to induction of inflammation [6], and upon verification of this via tissue damage assessment, we

therefore used this lobe for the molecular analysis of this study. For all experiments this model is used for (protein, histology, IF, etc.), dorsal-lateral prostates from six separate mice are used as separate data points.

### Protein Localization Via Immunohistochemistry

Prostate lobes were fixed in 10% formalin overnight, processed routinely, embedded in paraffin, and serially sectioned at 5 μm with a microtome. Tissues were subjected to heat-induced antigen retrieval in 10 mM citrate buffer (citrate buffer stock solution of monohydrate-free acid citric acid, sodium citrate dehydrate, pH 6.0) for 10 min. Sections were blocked at room temperature with a bovine serum albumin (BSA)-serum mixture for 2 hr and incubated with primary antibody overnight at 4°C. Primary antibodies and dilutions included BrdU labeling Detection kit II (1:20, Roche), rabbit anti-Cleaved Caspase 3 (1: 400, Cell Signaling Technologies, Danvers, MA), rabbit anti-Cleaved Caspase 7 (1:400, Cell Signaling Technologies), rabbit anti-Cleaved Caspase 9 (1:400, Cell Signaling Technologies), rabbit anti-survivin (1:100, Cell Signaling Technologies), rabbit anti-LC3 (1:200, Cell Signaling Technologies), and mouse CD45 (1:100, Cell Signaling Technologies). Sections were washed with PBS (Phosphate-buffered saline)-Tween and incubated with IgG Alexa 488 and IgG Alexa 594-conjugated secondary antibody against rabbit or mouse for 1 hr at room temperature (1:100, Invitrogen), followed by 10 min incubation with Hoechst 33258 nuclear stain (1 μg/ml). Tissues were washed and covered with an aqueous medium and glass coverslips. The sections were analyzed by immunofluorescence and the number of positive- and negative-stained cells was determined.

### Protein Quantification Via Immunoblotting

Prostate tissues were homogenized in lysis buffer containing protease inhibitor (150 mM NaCl, 10 mM tris, 1 mM EDTA, 1 mM benzenesulfonyl fluoride, and 10 μg/ml each of aprotinin, bestatin, L-luecine, and pepstatin A) and 1% Triton X-100. The homogenate was centrifuged for 20 min at 14,100*g* at 4 °C and the supernatant was collected and total protein concentration was determined by BCA (bicinchoninic acid) assay (Pierce, Rockford, IL). A total of 20 μg/well of Protein were resolved by electrophoresis in 4–15% gradient polyacrylamide gels. Proteins were transferred to polyvinylidene difluoride membranes, blocked for 24 hr [(10% Dry milk, 5% BSA, 0.05% $NaN_3$) in 1xPBS(2.7 mM KCl, 1.5 mM $KH_2PO_4$, 136 mM NaCl, 8 mM $Na_2HPO_4$)-Tween 20] and incubated overnight with one of the following primary antibodies: mouse β-actin (1:1000, Cell Signaling Technologies), rabbit survivin (1:1000, Cell Signaling Technologies), rabbit Bcl-2 (1:1000, Cell Signaling Technologies), rabbit Mcl-1 (1:500, Cell Signaling Technologies), and rabbit LC3 (1:1000, Cell Signaling Technologies). After blots were washed six times with PBS-Tween, blots were incubated with donkey antibody against rabbit immunoglobulin G conjugated to horseradish peroxidase for 1 hr (1:200,000 dilution, Pierce) in nonfat dry milk, PBS, and 0.05% Tween 20. Peroxidase activity was detected via West Femto chemiluminescence reagent (Pierce). Photo images were analyzed by densitometry.

### Cell Death/Survival Factors Expression Via ELISA

Prostate tissues were harvested and homogenized from 8-week-old C57BL/6J WT mice 0–14 days after uropathogenic *E. coli* strain 1677 instillation. For release experiments, tissues were equilibrated for 1 hr in aerated Krebs physiological salt solution, with buffer changes of 15 min and then 30 min. Krebs was collected after the experiment and frozen as the "released fraction." Additional tissues were harvested for the total tissue content, and these tissues were snap frozen in liquid nitrogen, placed in sterile PBS, and homogenized. Tissue slurries were centrifuged at 14,000*g* for 10 min and the supernatant was collected as the total tissue content fraction. All collections were analyzed by ELISA for TNF, TWEAK, TRAIL, FAS-Ligand, Shh, IGF-α, IL-1β, IL-6, TGF-β1, and TGF-β3 as recommended by the manufacturer (Biosource; Camarillo, CA). Absorbance readings for each concentration were normalized as a ratio to control non-inflamed prostates. Comparisons between inflammatory time points are expressed as mean ± s.e.m. $^{*}P < 0.05$ versus PBS-instilled prostate; using analysis of variance (ANOVA).

### DNA Fragmentation Via TUNEL

Prostate lobes were fixed in 10% formalin overnight, processed and embedded in paraffin and serially sectioned at 5 μm with a microtome and rehydrated as previously mentioned. Tissue sections were incubated with Proteinase K working solution (10 μg/ml in 10 nM Tris/HCl, pH 7.4–8) at RT for 15 min and then rinsed twice with PBS. Fifty microlitre of TUNEL reaction mixture (In Situ Cell Death Detection Kit Fluorescein, Roche Applied Science) were added to each section and slides were placed in a humidified atmosphere for 60 min at 37°C in the dark. The slides were then rinsed three times with

PBS and stained with Hoechst 33,258 as previously described. Tissues were then washed and covered with an aqueous medium and glass coverslips. Samples were directly analyzed under a fluorescence microscope using an excitation wavelength in the range of 450–500 nm and detection in the range of 515–565 nm (green).

### Human Specimens

Human specimens were obtained with appropriate minimal risk institutional review board approval according to the approval and guidelines at Indiana University School of Medicine. Sections were cut from pre-existing paraffin-embedded human prostate tissues obtained as part of a transurethral resection of the prostate (TURP), a prostatectomy, or from prostate specimens removed collaterally from bladder cancer patients undergoing radical cystectomy (cystoprostatectomy) as control human specimens. These controls were age-matched to the BPH-TURP and prostate cancer specimens, and were verified by record to be naïve for infection or pretreatment with Bacillus Calmette-Guérin as first-line therapy because these patients had presented with muscle invasive bladder cancer. Further, the controls were not exhibiting benign prostatic hyperplasia symptoms and were verified by pathology to be prostate cancer free. Control regions from both the transition zone and peripheral zone were used for analysis as controls for both BPH and prostate cancer, respectively. There were prostates collected from 12 separate patients used for this study. For calculation, five random 20× views were analyzed for survivin and CD45 positive cells and averaged for each separate data point. The age range of specimens is 45–72, with the average age of 64 for BPH specimens, 66 for control prostates, and 68 for prostate cancer specimens. Prostate cancer specimens were all Gleason 3+3, 3+4, or 4+3. All human specimens were stained with survivin and CD45 antibodies for immunofluorescence, as described above.

## RESULTS

### Inflammation Causes Tissue Damage and Hyperplasia in a Model of Prostatic Inflammation

Mice instilled with uropathogenic *E. coli* 1677 exhibited widespread inflammation with varying degrees of hyperplasia and dysplasia consistent with previous papers on this model, and as has been previously published, the dorsolateral lobe of the prostate produced the most consistent and dynamic response to inflammation [6,16]. Three days after instillation, WT animal epithelium develops distinct multilayers and display extensive inflammatory infiltrate (Fig. 1). Previous reports from this model indicate that the inflammatory infiltrate in this model is primarily neutrophilic 1–2 days post induction, and lymphocytic 3–5 days after inflammation with accompanying macrophages [6,16]. This phase mimics what is observed in human prostates with chronic inflammation [17,18]. Intense loci of inflammation are juxtaposed to epithelial hyperplasia and the prostatic glands juxtaposed to intense inflammation show tremendously increased epithelial cell proliferation and hyperplasia. Mice exhibiting 1–3 days of inflammation exhibit numerous damaged and apoptotic cells as evidenced by pyknotic nuclei and retracted

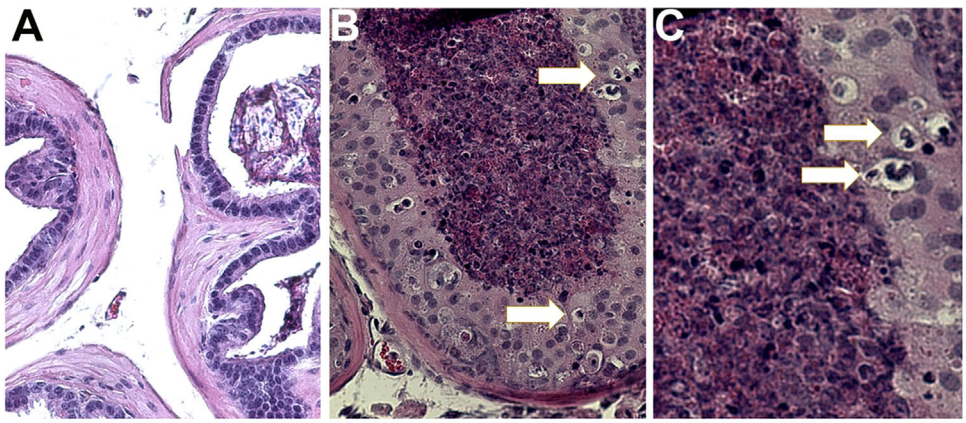


**Fig. 1.** Hematoxylin and Eosin staining of 3 day inflamed dorsolateral prostates in the mouse prostatic inflammation model. **A**: (200×) Non-inflamed control prostate shows pseudostratified epithelium and very few apoptotic or autophagic cells. **B**: 200× Inflamed prostatic duct shows layering of epithelium characteristic of reactive hyperplasia during inflammation, but also shows numerous damaged and apoptotic cells as evidenced by pyknotic nuclei and retracted cytoplasm (arrows). **C**: 400× Image of damaged epithelial cells in hyperplastic epithelium in inflamed prostate.

cytoplasm (Fig. 1). These data demonstrate that our model of prostatic inflammation is associated with the damaging effects of inflammation and cellular damage.

### Inflammation Causes Rapid Apoptotic Response

To characterize inflammation-induced apoptosis, we assessed control and inflamed mouse prostates for expression of executioner caspase 3, 7, and 6 cleavage via immunohistochemistry (Fig. 2A and B). We found an increase in cells exhibiting activation (cleavage) of all three executioner caspases with caspase 3 being the most dramatic, peaking at day 2 with 1.3% of cells expressing cleaved caspase 3 (n = 6 mice). Cleaved caspase 3 positive cells were primarily found in select basal and luminal epithelial cells of prostatic glands and absent from the fibromuscular stroma. In addition, we assessed these tissues for later stage apoptosis by staining for nick-end labeling of fragmented DNA. To determine this, a terminal deoxynucleotidyl transferase dUTP nick-end labeling (TUNEL) was performed to measure percent of epithelial cells in later stage apoptosis as described in histologic sections of prostate tissue and positive cells were detected by fluorescent microscopy (Fig. 2C). Few fluorescein-positive cells were found in days 0 and 1 of infection but a significant increase in apoptotic cells

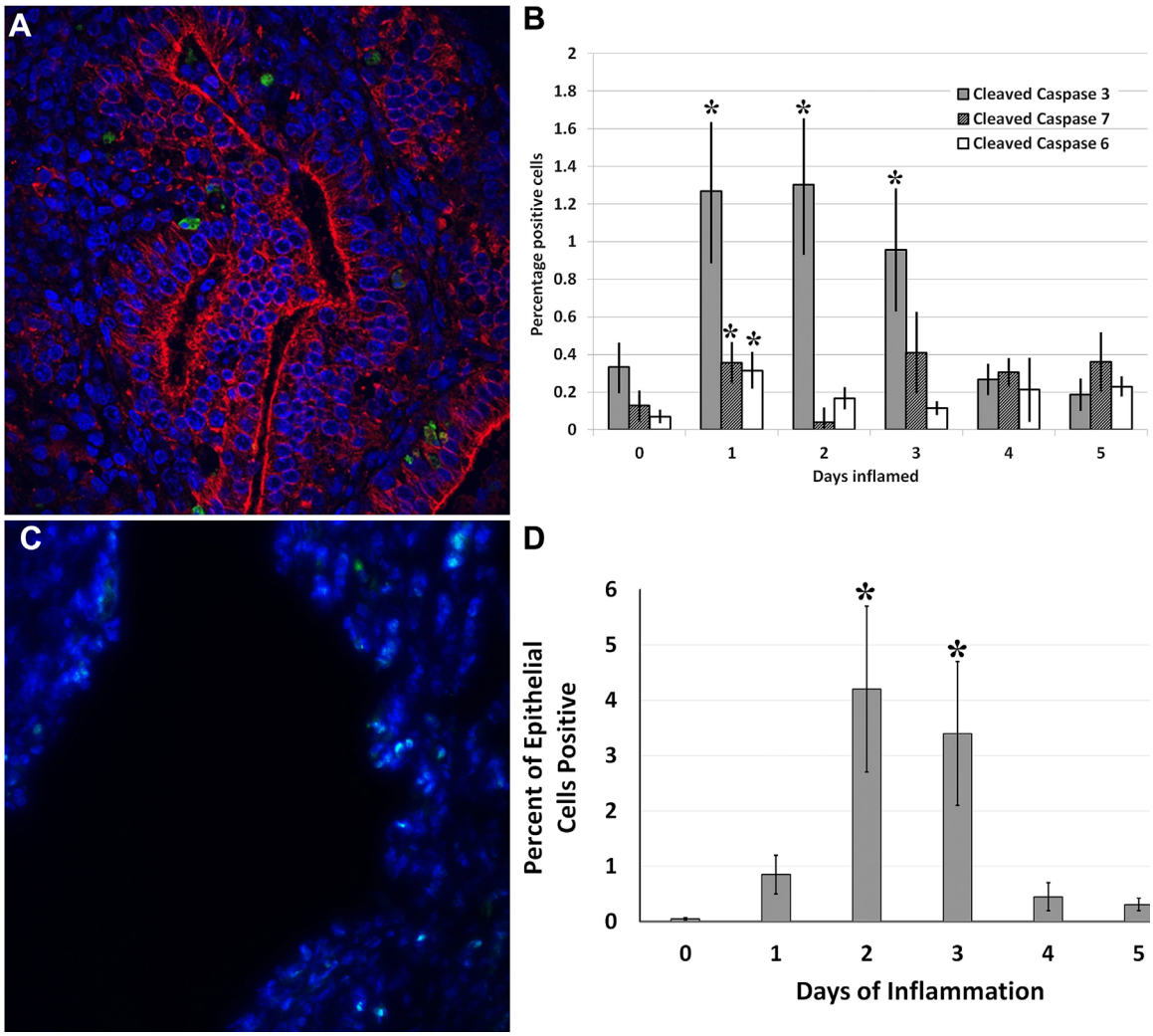


**Fig. 2.** Inflammation of the mouse prostate results in induced apoptotic signaling. **A**: Fluorescent image (200×) of cleaved caspase 3 (green) in the epithelium (PanCK-red) of mouse prostates inflamed 3 days. **B**: Calculated data of epithelial cells for cleaved caspases 3, 7, and 6 from 6 mouse dorsal-lateral prostate lobes inflamed to the time points shown, expressed as percentage of cleaved caspase-positive cells within the epithelial compartment. **C**: Fluorescent image (200×) of TUNEL-positive cells. **D**: Calculated data of epithelial cells for TUNEL from 6 mouse dorsal-lateral prostate lobes inflamed to the time points shown, expressed as percentage of TUNEL-positive cells within the epithelial compartment. All data are expressed as mean ± s.e.m. $^{*}P < 0.05$ versus PBS-instilled prostate; comparisons using analysis of variance (ANOVA), n = 6.

was found in day 2 with subsequent decrease by day 4. The fluorescein positive cells, like the caspase 3 positive cells, were primarily found in the basal and luminal compartments of the prostatic glands.

### Inflammation Induces Death and Survival Factor Production and Release

Inflammation induces coordinated and temporal expression and release of known cell death factors, subsequently followed by an induction of a panel of known cell survival-inducing factors. As measured by ELISA, bona fide cell death-inducing mediators TNFα, TWEAK, TRAIL, and FAS ligand are all induced rapidly and transiently upon induction of acute inflammation in the dorsolateral prostate, maximizing at 1–2 days after induction (Fig. 3A and B). Subsequent to induction of death ligands, the production of known cell survival factors Shh, IGF-1, IL-1α, IL-6, TGFβ1, and TGFβ2 are substantially induced in the second day of inflammation, and maximizes at day 3 (Fig. 3C and D, n = 6 mice). IL-1α, IL-6, and TGFβ1 remained significantly induced for 5 days after inflammation induction. These data demonstrate that death factors coincide with the acute and neutrophilic phase of inflammation, and are coordinately followed by the induction of survival factors corresponding to the lymphocytic phase of inflammation.

### Inflammation Induces Cell Survival Signaling Pathways in Response to Apoptotic Signals

We assessed the induction of four previously identified survival signaling molecules, previously known to regulate cell survival in prostate cells: survivin, Bcl-2, Bcl-XL, and Mcl-1 (Fig. 4). Our data

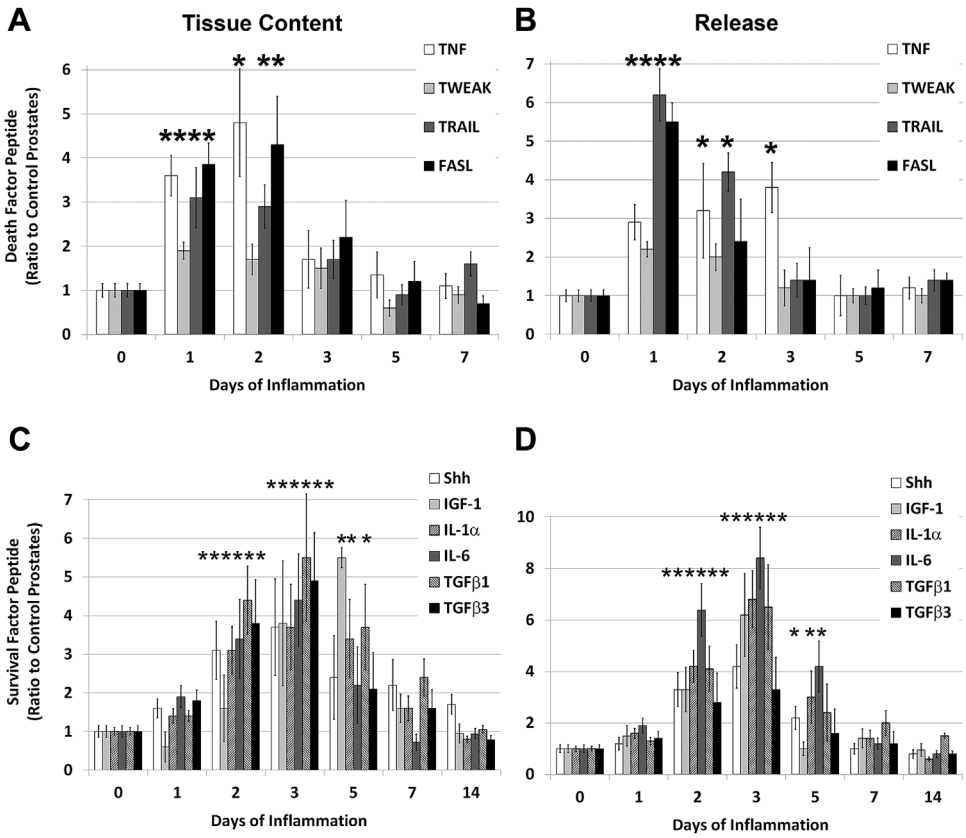


**Fig. 3.** Inflammation induces the expression and release of known cell death factors, followed by an induction of a panel of known cell survival-inducing factors. **A**: Total tissue content of TNFα, TWEAK, TRAIL, and FAS ligand are all induced rapidly upon induction of inflammation in the dorsolateral prostate, maximizing at 1–2 days after induction. **B**: Correspondingly, the released fraction of these death ligands increases, indicating that release of the factor occurs allowing their function. **C**: Subsequently, the induction of known cell survival factors Shh, IGF-1, IL-1α, IL-6, TGFβ1, and TGFβ2 begins in the second day of inflammation, and maximizes at day 3. IL-1α, IL-6, and TGFβ1 remained induced for 5 days after inflammation induction. **D**: The released fraction of cell survival factors increases correspondingly to their production. All peptides were assessed by ELISA of whole dorsolateral prostate lobes and calculated as picogram of peptide per gram of tissue. Data were then normalized as a ratio to control non-inflamed prostates at the given time point of induction, for presentation. All data are expressed as mean ± s.e.m. $^{*}P < 0.05$ versus PBS-instilled prostate; comparisons using analysis of variance (ANOVA), n = 6. Asterisk-labeled time points are those that show significant inducibility of all death or survival factors.

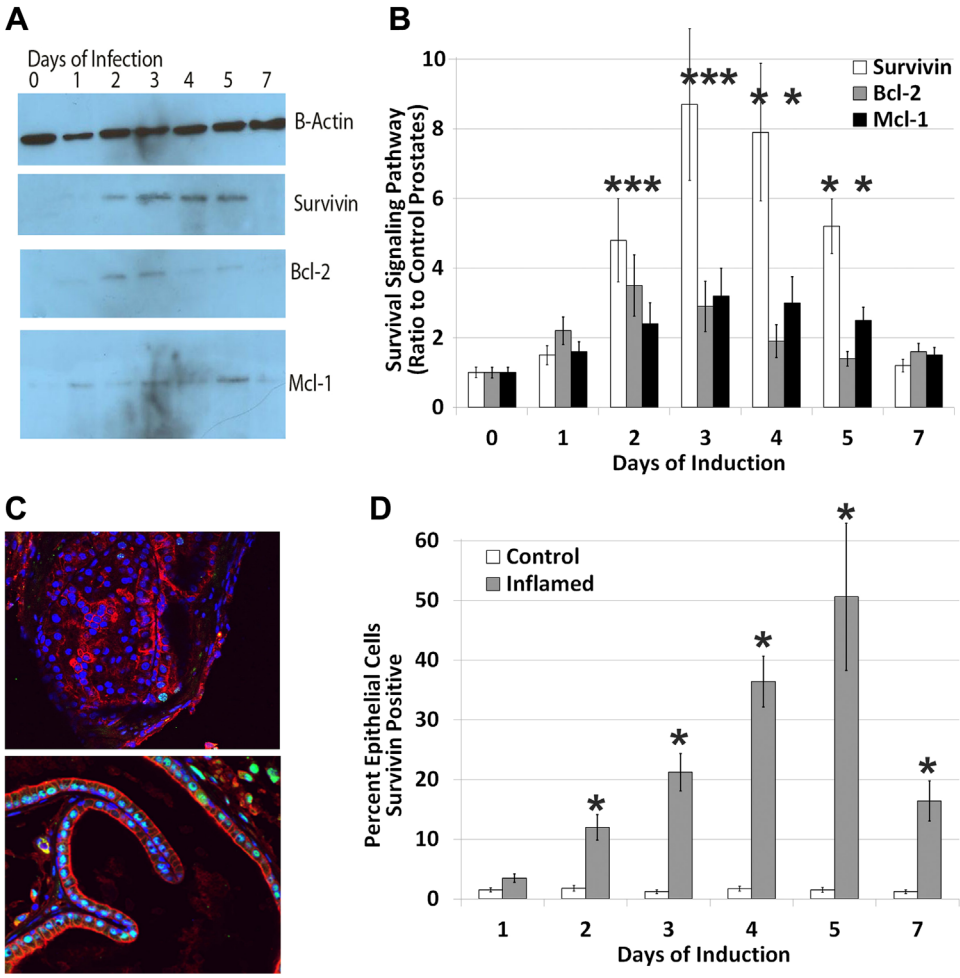


**Fig. 4.** Inflammation induces three primary cell survival signaling pathways in mouse dorsolateral prostates, most prominently, survivin. **A**: Immunoblot example of induction of survivin, Bcl-2, and Mcl-1 during the time course of inflammation in mouse prostates. **B**: Quantified data of relative expression of all three survival proteins during prostatic inflammation; data were calculated as ratio of pixel intensity of the given survival protein, relative to β-actin, and expressed as ratio of expression to control prostates at the corresponding time of induction. Data are expressed as mean ± s.e.m. $^{*}P < 0.05$ versus PBS-instilled (control) prostate; comparisons using analysis of variance (ANOVA), n = 6. **C**: Immunofluorescence of survivin expression (green) in 5 day instilled control (top) and inflamed (bottom) dorsolateral prostates demonstrating epithelial cell (PanCK, red) expression in the nucleus during inflammation. **D**: Quantified cell counting of epithelial cells positive for survivin expression; data expressed are the percentage of epithelial cells expressing survivin in control and inflamed prostates at each time point of inflammation. All data are expressed as mean ± s.e.m. $^{*}P < 0.05$ versus PBS-instilled prostate; comparisons using analysis of variance (ANOVA), n = 6.

indicate that inflammation induces the expression of survivin, Bcl-2 and Mcl-1, but had no effect on Bcl-XL expression (Not shown). The most prominently induced survival protein by inflammation was survivin, exhibiting an eightfold induction at days 3 and 4 after inflammation relative to uninflamed control prostates (Fig. 4A and B; n = 6 mice). Since survivin was the most dynamic and consistently induced survival factor in inflamed prostates, we sought to further characterize its induction. Survivin is rarely expressed in control prostates, being expressed in 1% of epithelial cells, and primarily in select basal cells (Fig. 4C-top). Immunofluorescence of survivin expression increased linearly by day throughout the first 5 days of inflammation (Fig. 4D), and by 5 days 50% of the epithelial cells of inflamed prostates were positive for survivin (Fig. 4D), image depicted in Figure 4C-bottom. The percentage of survivin-positive cells remained increased for 7 days of infection. These data indicate that survival proteins are induced during prostatic inflammation, corresponding to induced survival factor signals and the lymphocytic phase of inflammation, and temporally following the neutrophilic death factor/apoptotic phase.

### Inflammation Induces Autophagy: LC 3 Association With the Autophagosome

As autophagy is a cell mechanism that can lead to either cell survival or cell death, we sought to characterize its induction in prostatic inflammation. Inflammation increases both the expression and vesicle association of the autophagy LC3 (Fig. 5). LC3 is expressed in the cytosol of cells and, upon initiation of autophagy, LC3 associates with vesicular membranes to form the autophagosome. This causes LC3 to run faster on gels, so a lower running band in immunoblotting is indicative of autophagosome-associated LC3, and therefore autophagy induction. Immunoblotting of proteins from inflamed prostates demonstrates that autophagy is induced by inflammation in the prostate, maximizing at 3 days of inflammation (Fig. 5A and B; n = 6 mice). Additionally, LC3 expression itself is also induced after three days of inflammation. To further characterize LC3 during prostatic inflammation, we assessed tissue localization by in immunofluorescence. Autophagosome-associated LC3 is associated with a punctate appearance as the protein is concentrated around the vesicle (Fig. 5C). We found that the number of prostatic epithelial cells exhibiting punctate LC3 increased from 4% of epithelial cells to 25% by the third day of inflammation

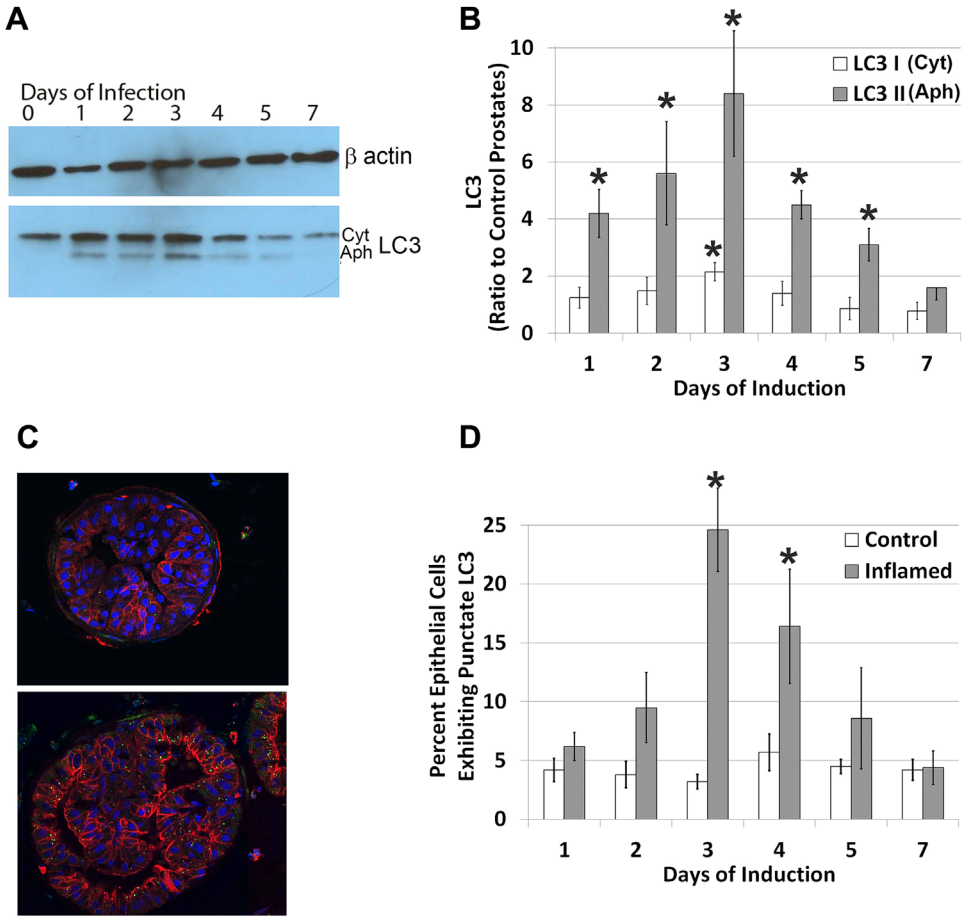


**Fig. 5.** Inflammation autophagy marker expression in mouse dorsolateral prostates. **A**: Immunoblot example of induction of the autophagy marker LC3 at inflammation time points indicated; the higher running band (cyt) represents cytosolic LC3 while the lower running band (Aph) indicates LC3 associated in the autophagasome, and is indicative of autophagy induction. **B**: Quantified data of relative expression of all cytosolic and autophagasome-associated LC3; data were calculated as ratio of pixel intensity of the LC3 form, relative to β-actin, and expressed as ratio of expression to control prostates at the corresponding time of induction. Data are expressed as mean ± s.e.m. $^{*}P < 0.05$ versus PBS-instilled (control) prostate; comparisons using analysis of variance (ANOVA), n = 6. **C**: Immunofluorescence of LC3 (green) localization in 3 day instilled control (top) and inflamed (bottom) dorsolateral prostates demonstrating the characteristic punctate LC3 Localization with the autophagasome of autophagic epithelial cells, a further indicator of autophagic cells (PanCK, red). **D**: Quantified cell counting of epithelial cells positive for punctate LC3 Localization; data expressed are the percentage of epithelial cells expressing punctate LC3 in control and inflamed prostates at each time point of inflammation. All data are expressed as mean ± s.e.m. $^{*}P < 0.05$ versus PBS-instilled prostate; comparisons using analysis of variance (ANOVA), n = 6.

(Fig. 5D). Autophagic cells were found throughout the epithelium, in both luminal and basal layers. These data demonstrate that the potentially cell survival mechanism of autophagy is induced by acute prostatic inflammation, and maximizes during the lymphocytic phase.

### Survivin Is Induced Juxtaposed to Inflammation in Human Prostate Specimens

In our in vivo mouse model of prostatic inflammation, survivin is the most consistently induced survival factor in the prostate in response to inflammatory signals. Because of this, we sought to determine if it is induced by inflammation in human prostate specimens. To address inflammation and survival protein expression in human tissue, we co-stained for $CD45^+$ (immune cells) and survivin in non-diseased (prostates removed from cystectomies), BPH specimens (via TURP), and prostate cancer specimens (removed via prostatectomy), 12 tissues (from 12 separate patients) per group. As previously reported, survivin is induced in the majority of prostate cancer specimens, and is not expressed in the majority of non-diseased control prostates. However, our staining also demonstrated that regions of inflammation associated with survivin induction regardless of whether the region was found in non-diseased or diseased prostates (Fig. 6). We defined both inflamed and non-inflamed regions in all three prostatic conditions (non-diseased, BPH, and cancer) by the number of CD45-evident 20× fields. Based on our previously established mouse model inflammatory scoring [6], we set the criteria for inflammation to be greater than or equal to 30 $CD45^+$ cells per 20× field, and non-inflamed regions were defined as less than 10 $CD45^+$ cells per field. Using this criteria, we quantified the number of survivin-positive cells in sections from inflamed and non-inflamed regions in non-diseased, BPH, and cancerous prostate specimens. We found that regardless of condition, inflamed fields were associated with 60–70% of epithelial cells positive for survivin, while non-inflamed non-diseased and BPH fields exhibited less than 10% of epithelial cells positive for survivin, and non-inflamed cancerous fields were associated with 24% positive cells (Fig. 6B). While there was a threefold increase in survivin-positivity among prostate cancer specimens independent of inflammation, the primary difference between diseased and non-diseased prostates was the prevalence of inflammation (Fig. 6C). In non-diseased prostates, severe inflammation represented on average 11% of sections, while in BPH and prostate cancer sections severe inflammation constituted 82% and 71% of the section, respectively. There was no difference in the severity of inflammation in the 20× views quantified in this study once they were determined to be in the "severe" (>30 CD45-positive leukocytes per field) category. Additionally, we observed no significant difference in survivin-positivity between the transition zone and peripheral zone of non-diseased prostates.

## DISCUSSION

Inflammation is a common feature of prostate biology and is believed to be associated with the disease progression involved in both BPH and prostate cancer. Yet, inflammation is also a destructive process that involves a repair and recovery stage in which protected cells must survive the initial insults of inflammation, followed by their rapid proliferation as a means to repopulate the damaged tissue. The cell signaling mechanisms involved in coordinating these events is not understood, and little is known as to how the epithelium of tubular structures such as the prostate protects the specialized cells that are the keystones of epithelial repair and recovery.

The data in the present study indicate that inflammation induces a profile of cell death and cell survival-inducing factors, coordinated such that death factors and induction of cell death cellular mechanisms occurs within the first 48 hr after induction of inflammation, followed by a maximized expression of survival factors and signaling pathways. Inflammation causes visible death of the prostatic epithelium in the first 48 hr of inflammation as evidenced by H&E staining and confirmed by activation of caspases and nick-end labeling. Coordinate with this, there is a significant induction of cell death factors including TNFα, TWEAK, TRAIL, and FasL. Secondary to cell death, the acute inflammation time course exhibits induction of known survival factors including growth factors, cytokines, and developmental morphogens that correspond to activation of survival pathways that include survivin, Mcl-1, and Bcl-2. We conclude from this that a population of epithelial cells resides in the prostatic epithelium that responds to inflammatory signals by inducing survival factors, and functions to repopulate the tissue during repair secondary to the damaging effects of inflammatory triggers.

Additionally, autophagy mechanisms maximize during this survival phase and may represent an additional cell survival mechanism in prostatic epithelial cells. Autophagy is indicated by the formation of autophagosomes for cell protein digestion during stress. Cells in autophagy can either use the digested material for survival, or they can be entered into the apoptotic cascade if the stress time period endures. During the induction of autophagy, the normally

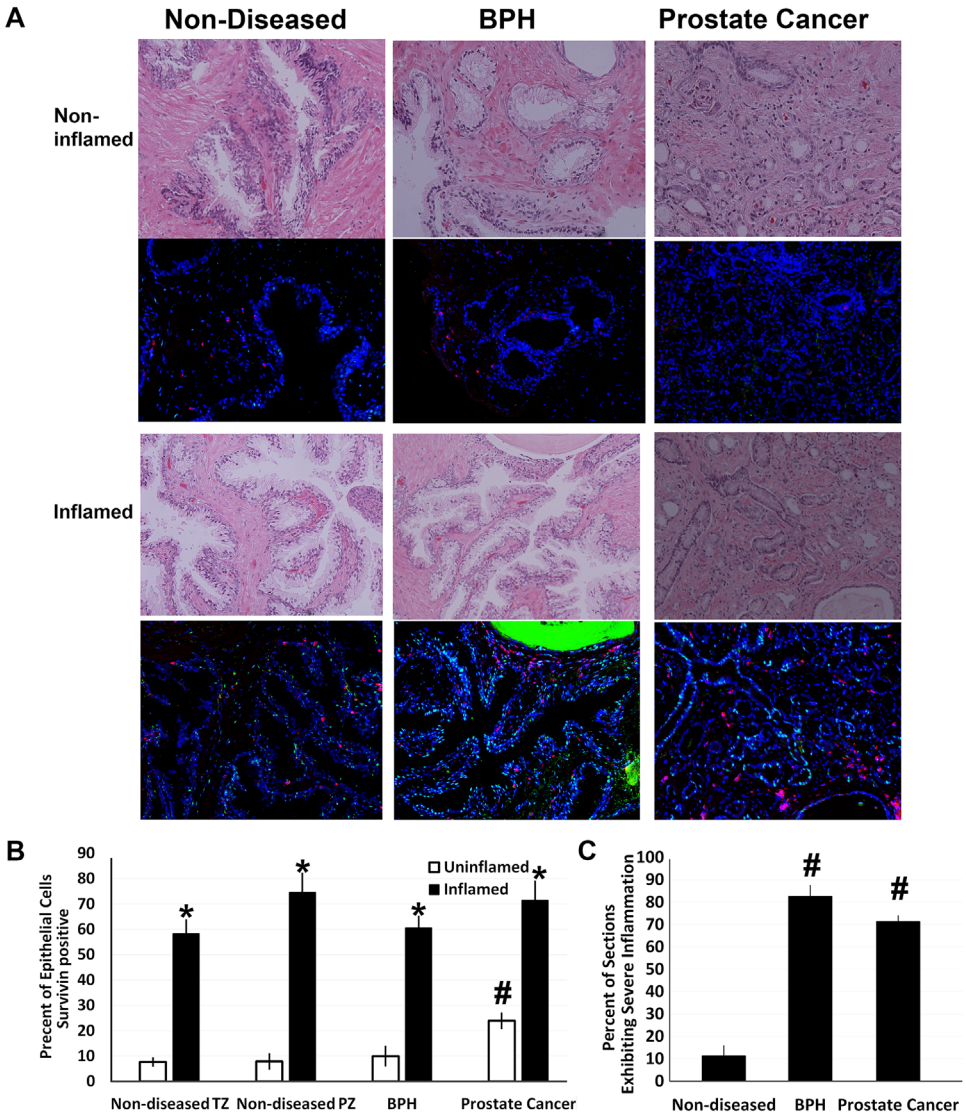


**Fig. 6.** Human prostate specimens demonstrate intense survivin staining juxtaposed to regions of inflammation. **A**: Immunofluorescent images of non-inflamed or inflamed human prostates representing non-diseased controls (peripheral zone) taken from cystoprostatectomy cancer and BPH-free prostate specimens, BPH specimens (transition zone from TURP), or prostate cancer specimens, as indicated. Sections were stained for survivin (green) and CD45, a pan leukocyte marker (red) to identify regions of inflammation. Sections were deemed non-inflamed if they exhibited less than 10 Leukocytes per 20× field, and inflamed if they exhibited greater than 30 Leukocytes per field. **B**: Quantified cell counting of epithelial cells positive for survivin expression in human prostates; data expressed are the percentage of epithelial cells expressing survivin in non-inflamed and inflamed prostates at each time point of inflammation—three 20× fields per prostate section were averaged for each data point, and all data are expressed as mean ± s.e.m. $^{*}P < 0.05$ inflamed versus non-inflamed prostate; $\#P < 0.05$ disease condition versus non-diseased control. Analysis of variance (ANOVA), n = 12 human prostates. **C**: percent of sections from each human prostate group (non-diseased, BPH, and cancer) that exhibited 30 Leukocytes per 20× section. Three 20× fields per prostate section were averaged for each data point, and all data are expressed as mean ± s.e.m. $^{\#}P < 0.05$, disease condition versus non-diseased control. Analysis of variance (ANOVA), n = 12 human prostates.

cytosolic protein Light Chain 3 (LC3) associates and participates in the formation of the autophagosome. As such, the association of LC3 in a lipid fraction—that of a membrane—indicates the induction of autophagy. In our study, autophagosome-associated LC3 was evident by two methods: the faster-running band at 14 KD in immunoblotting that indicates autophagosome association; secondly, the specific exhibition of LC3 into punctate formations indicating the presence of autophagosomes. Our data demonstrate a substantial increase in the faster running band by immunoblotting, and in the number of epithelial cells exhibiting punctate LC3 containing autophagosomes. From this we conclude that inflammation

induces autophagy in a subset of prostate epithelial cells in experimental models of prostatic inflammation.

The mouse model used in this study is a model of acute inflammation that progresses to chronic inflammation. This is characterized by an early neutrophilic infiltrate that dominates in the first 2 days of induction, and progresses to a primarily lymphocytic and monocytic infiltrate in days 3–5. This later lymphocytic chronic stage of the inflammatory response has a cellular infiltrate and an expression profile consistent to what is observed in human chronically inflamed prostates. The time course of cellular infiltrate in this model exhibits remarkably little experimental variation error, demonstrating that the time course of the inflammatory response is highly reproducible and consistent. Further, inflammation in this model was accompanied by increased expression of several inflammatory mediators and gene products including IL-1 family members, IL-6, COX-2, IGF-1, and FGFs, commonly observed in chronic prostatic inflammation. Therefore it is not unexpected that an increase in survival protein expression occurs during the chronic phase of this model, just as is observed in human chronically inflamed prostates.

Survivin was the most consistent and substantially induced of the survival proteins in our mouse study, and we sought to validate its responsiveness to inflammation in human specimens. While the expression of survivin is well-known to be induced in both BPH and prostate cancer [19–21], this is the first report we are aware of in which survivin localization is characterized juxtaposed to inflammation. We found that survivin expression does localize to areas of severe inflammation, but what was striking is how this localization is largely disease-independent. There was no difference in the number of survivin-positive cells in inflamed regions between BPH, cancer, and non-diseased regions; the primary discriminating factor between the pathological states is how widespread inflammation is in each state. Severe inflammation was present in over 80% of our BPH sections and over 70% of our prostate cancer specimens, but was only a feature in less than 15% of non-diseased sections. Inflammation was associated with reactive hyperplasia and stromal desmoplasia in all tissues where it was present, but there was no consistent formation of any pre-malignant epithelial lesions such as dysplasia in inflamed regions of non-diseased prostates. We propose that the previously published findings describing high survivin localization in diseased prostates is in large part a factor of the increased inflammation in those specimens. It must be noted, however, that in those uncommon regions of prostate cancer that are not associated with inflammatory infiltrate, there is still an increased number of survivin-positive cells, independent of inflammation. Therefore we conclude that prostate cancer does have intrinsic survivin induction relative to benign epithelium, but this is still enhanced with inflammation. BPH specimens did not exhibit any increase, absent of inflammation.

There is a clear association of BPH with inflammation, both in proliferating cells and in association with symptoms. The prevalence of inflammation in BPH specimens is repeatedly reported to be found in between 75% and 100% of specimens. A well-characterized study by Nickel et al. reported substantial prostatic inflammation in 100% of 80 men undergoing prostatectomy for treatment of BPH [22], and histological examination of prostates from 8224 men enrolled in the REDUCE trial revealed inflammation in 78% of specimens [23]. Critically, histologically verified inflammation is the most tightly correlated histological finding to prostate symptomology in men with BPH [24]. Similarly, strong evidence links inflammation to the development, growth, and survival of cancer in the prostate [1]. Histopathology studies of human prostatectomy specimens identified lesions characterized by proliferating epithelial cells and activated inflammatory cells (proliferative inflammatory atrophy, PIA) in juxtaposition to areas of neoplasia. Sustained cell proliferation in the inflammatory environment rich in growth factors, activated stroma, and DNA-damage-promoting agents, could potentiate, and/or promote neoplasia. Additionally, proliferative inflammatory atrophy (PIA) is characterized by proliferating epithelial cells and is found in association with prostatic intra-epithelial neoplasia (PIN) and prostate cancer. These findings have prompted the hypothesis that chronic inflammation is involved in the genesis and/or progression of prostate cancer.

Several aberrant molecular mechanisms in apoptosis pathways have been identified to result in prostate disease, and androgen axis modulators—a mainstay of our therapies against prostate cancer growth—rely heavily on induction of apoptotic mechanisms for their efficacy [25–28]. Multiple modifications to cell death and survival pathways have been discovered in prostate tumors, BPH, and prostate cell lines that may participate in either tumorigenesis, proliferation, or therapy resistance. Increased expression of the survival proteins survivin, Bcl-2, Bcl-xL, Bcl-ω, and Mcl-1 are associated with prostate cancer and BPH, and interestingly inhibiting their expression sensitizes cells to cytotoxic therapies [29–31]. In addition, downregulation or inhibition of these survival proteins results in increased chemosensitivity in prostate cell lines [31–33]. Finally, prostate cancer cells exhibit decreased death receptor expression and upregulated decoy death receptor expression, and this results in

diminished apoptosis induction capacity [34,35]. Our present findings add to the understanding of the balance between pro-apoptotic and pro-survival signaling in prostate epithelial cells by demonstrating extrinsic control of both death factors and subsequent survival factor induction in a specialized cell population, by inflammation.

## CONCLUSION

Our data indicate that prostatic tissue responds to the damaging effects of inflammation by an active induction of cell survival factors and signaling mechanisms, most notably survivin. Autophagy, a potential cell survival mechanism, is also substantially activated and these survivin-expanded cells may depend upon survival signaling. This study further suggests that there is a coordinated induction of survival factors that function to protect and expand a specialized set of prostatic epithelial cells. In human prostate, induction of survivin is juxtaposed to loci of severe inflammation induction in benign and cancerous prostates, and inflammation appears to be more acutely the inducer of this critical protein in the microenvironment than cancer itself is. Future studies will be aimed at determining if early stage prostate cancer set in inflammatory microenvironments survive the damaging effects of inflammation using these mechanisms.

## AUTHORS' CONTRIBUTIONS

McIlwain, Zoetemelk, Myers, and Jerde participated in research design. Experiments was conducted by McIlwain, Zoetemelk, Myers, Edwards, Snider, and Jerde. McIlwain, Zoetemelk, Edwards, Snider, Myers, and Jerde performed data analysis. McIlwain, Snider, and Jerde wrote and contributed to the writing of the manuscript.

## ACKNOWLEDGMENTS

The authors gratefully acknowledge Jill Fehrenbacher, Kai-Ming Chou and Yeh-Wen Chen for use and expertise in fluorescent microscopy. This work was funded by National Institutes of Health-NIDDK [DK092366-01A1], the Department of Pharmacology and Toxicology, the Indiana University School of Medicine Melvin and Bren Simon Cancer Center, Indianapolis, IN and Indiana Clinical and Translational Sciences Institute (CTSI) (DWM).

## REFERENCES

1. De Marzo AM, Platz E, Sutcliffe S, Xu J, Grönberg H, Drake CG, Nakai Y, Isaacs WB, Nelson WG. Inflammation in prostate carcinogenesis. Nat Rev Cancer 2007;7:256–269.
2. Kramer G, Mitteregger D, Marberger M. Is benign prostatic hyperplasia (BPH) an immune inflammatory disease? Eur Urol 2007;51:1202–1216.
3. Delongchamps NB, de la Roza G, Chandan V, Jones R, Sunheimer R, Threatte G, Jumbelic M, Haas GP. Evaluation of prostatitis in autopsied prostates—Is chronic inflammation more associated with benign prostatic hyperplasia or cancer? J Urol 2008;179(5):1736–1740.
4. Sfanos KS, De Marzo AM. Prostate cancer and inflammation: The evidence. Histopathology 2012;60(1):199–215.
5. Elkahwaji JE, Zhong W, Hopkins WJ, Bushman W. Chronic bacterial infection and inflammation incite reactive hyperplasia a mouse model of chronic prostatitis. Prostate 2007;67(1):14–21.
6. Boehm BJ, Colopy SA, Jerde TJ, Loftus CJ, Bushman W. Acute bacterial inflammation of the mouse prostate. Prostate 2012; 72(3):307–317.
7. Cohen RJ, Shannon BA, McNeal JE, Shannon T, Garrett KL. Propionibacterium acnes associated with inflammation in radical prostatectomy specimens: A possible link to cancer evolution? J Urol 2005;173(6):1969–1974.
8. Sfanos KS, Sauvageot J, Fedor HL, Dick JD, De Marzo AM, Isaacs WB. A molecular analysis of prokaryotic and viral DNA sequences in prostate tissue from patients with prostate cancer indicates the presence of multiple and diverse microorganisms. Prostate 2008;68(3):306–320.
9. Sfanos KS, Isaacs WB. An evaluation of PCR primer sets used for detection of Propionibacterium acnes in prostate tissue samples. Prostate 2008;68(14):1492–1495.
10. Hochreiter WW, Duncan JL, Schaeffer AJ. Evaluation of the bacterial flora of the prostate using a 16S rRNA gene based polymerase chain reaction. J Infect Dis 1999;180(4):1378–1381.
11. Puchelle E, Zahm JM, Tournier JM, Coraux C. Aiwary epithelial repair, regeneration, and remodeling after injury in chronic obstructive pulmonary disease. Proc Am Thorac Soc 2006;3: 726–733.
12. Wang W, Bergh A, Damber JE. Chronic inflammation in benign prostate hyperplasia is associated with focal upregulation of cyclooxygenase-2, Bcl-2, and cell proliferation in the glandular epithelium. Prostate 2004;1:60–72.
13. Codogno P, Meijer AJ. Autophagy and signaling: Their role in cell survival and cell death. Cell Death Differ 2005;12:1509–1518.
14. Yang ZJ, Chee CE, Huang S, Sinicrope FA. The role of autophagy in cancer: Therapeutic implications. Mol Cancer Ther 2011;10:1533.
15. Rodriguez-Enriquez S, He L, Lemasters JJ. Role of mitochondrial permeability transition pores in mitochondrial autophagy. Int J Biochem Cell Biol 2004;36:2463–2472.
16. Jerde TJ, Bushman W. IL-1 induces IGF-dependent epithelial proliferation in prostate development and reactive hyperplasia. Sci Signal 2009;2(86):49.
17. Theyer G, Kramer G, Assmann I, Sherwood E, Preinfalk W, Marberger M, Zechner O, Steiner GE. Phenotypic characterization of infiltrating leukocytes in benign prostatic hyperplasia. Lab Invest 1992;66(1):96–107.
18. Robert G, Descazeaud A, Nicolaïew N, Terry S, Sirab N, Vacherot F, Maillé P, Allory Y, de la Taille A. Inflammation in benign prostatic hyperplasia: A 282 patients' immunohistochemical analysis. Prostate 2009;69(16):1774–1780.
19. Rodríguez-Berriguete G, Fraile B, de Bethencourt FR, Prieto-Folgado A, Bartolome N, Nuñez C, Prati B, Martínez-Onsurbe P, Olmedilla G, Paniagua R, Royuela M. Role of IAPs in prostate

cancer progression: Immunohistochemical study in normal and pathological (benign hyperplastic, prostatic intraepithelial neoplasia and cancer) human prostate. BMC Cancer 2010;10:18.

20. Nastiuk KL, Krolewski JJ. FLIP-ping out: Death receptor signaling in the prostate. Cancer Biol Ther 2008;7:1171–1179.
21. Shariat SF, Ashfaq R, Roehrborn CG, Slawin KM, Lotan Y. Expression of survivin and apoptotic biomarkers in benign prostatic hyperplasia. J Urol 2005;174(5):2046–2050.
22. Nickel JC, Downey J, Young I, Boag S. Asymptomatic inflammation and/or infection in benign prostatic hyperplasia. BJU Int 1999;84(9):976–981.
23. Nickel JC, Roehrborn CG, O'Leary MP, Bostwick DG, Somerville MC, Rittmaster RS. The relationship between prostate inflammation and lower urinary tract symptoms: Examination of baseline data from the REDUCE trial. Eur Urol 2008;54:1379–1384.
24. Nickel JC. Inflammation and benign prostatic hyperplasia. Urol Clin North Am 2008;1:109–115.
25. Yamamoto H, Ngan CY, Monden M. Cancer cells survive with survivin. Cancer Sci 2008;9:1709–1714.
26. Kishi H, Igawa M, Kikuno N, Yoshino T, Urakami S, Shiina H. Expression of the survivin gene in prostate cancer: Correlation with clinicopathological characteristics, proliferative activity and apoptosis. J Urol 2004;171:1855–1860.
27. De Nunzio C, Kramer G, Marberger M, Montironi R, Nelson W, Schröder F, Sciarra A, Tubaro A. The controversial relationship between benign prostatic hyperplasia and prostate cancer: The role of inflammation. Eur Urol 2011;1:106–117.
28. Cornforth AN, Davis JS, Khanifar E, Nastiuk KL, Krolewski JJ. FOXO3a mediates the androgen-dependent regulation of FLIP and contributes to TRAIL-induced apoptosis of LNCaP cells. Oncogene 2008;27:4422–4433.
29. Sun A, Tang J, Hong Y, Song J, Terranova PF, Thrasher JB, Svojanovsky S, Wang HG, Li B. Androgen receptor-dependent regulation of Bcl-xL expression: Implication in prostate cancer progression. Prostate 2008;68:453–461.
30. van Delft MF, Huang DC. How the Bcl-2 family of proteins interact to regulate apoptosis. Cell Res 2006;16:203–213.
31. Nguyen M, Marcellus RC, Roulston A, Watson M, Serfass L, Murthy Madiraju SR, Goulet D, Viallet J, Bélec L, Billot X, Acoca S, Purisima E, Wiegmans A, Cluse L, Johnstone RW, Beauparlant P, Shore GC. Small molecule obatoclax (GX15-070) antagonizes Mcl-1 and overcomes Mcl-1—Mediated resistance to apoptosis. Proc Natl Acad Sci USA 2007;104:19512–19517.
32. Sternberg CN, Dumez H, Van Poppel H, Skoneczna I, Sella A, Daugaard G, Gil T, Graham J, Carpentier P, Calabro F, Collette L. Lacombe D; EORTC Genitourinary Tract Cancer Group. Docetaxel plus oblimersen sodium (Bcl-2 antisense oligonucleotide): An EORTC multicenter, randomized phase II study in patients with castration-resistant prostate cancer. Ann Oncol 2009;20:1264–1269.
33. Mohammad RM, Goustin AS, Aboukameel A, Chen B, Banerjee S, Wang G, Nikolovska-Coleska Z, Wang S, Al-Katib A. Preclinical studies of TW-37, a new nonpeptidic small-molecule inhibitor of Bcl-2, in diffuse large cell lymphoma xenograft model reveal drug action on both Bcl-2 and Mcl-1. Clin Cancer Res 2007;13:2226–2235.
34. Bova GS, MacGrogan D, Levy A, Pin SS, Bookstein R, Isaacs WB. Physical mapping of chromosome 8p22 markers and their homozygous deletion in a metastatic prostate cancer. Genomics 1996;35:46–54.
35. Sanlioglu AD, Koksal IT, Ciftcioglu A, Baykara M, Luleci G, anlioglu SS. Differential expression of TRAIL and its receptors in benign and malignant prostate tissues. J Urol 2007;177:359–364.

**TITLE: APE1/Ref-1 Redox-Specific Inhibition Decreases Survivin Protein Levels and Induces Cell Arrest in Prostate Cancer Cells**

**AUTHORS:** David W. McIlwain,[1] Melissa L. Fishel,[1,2] Mark R. Kelley,[1,2] and Travis J. Jerde[1]

[1]Department of Pharmacology and Toxicology, Indiana University School of Medicine, Indianapolis, Indiana

[2]Department of Pediatrics, Wells Center for Pediatric Research, Indiana University School of Medicine, Indianapolis, Indiana

**KEYWORDS:** Prostate Cancer, APE1/Ref-1, Survivin, NFκB Signaling, Redox Regulation

**TOTAL NUMBER OF FIGURES/TABLES:** 7 Figures, 1 Table and 2 Supplementary Figures

## ABSTRACT

A key feature of prostate cancer progression is the induction and activation of survival proteins, most prominently the IAP family member, survivin. Apurinic/apyrimidinic endonuclease 1 redox factor 1 (APE1/Ref-1) is a multifunctional protein that has recently been found to be essential in activating oncogenic transcription factors. APE1/Ref-1 has been shown to be expressed in human prostate cancer, therefore we sought to characterize APE1/Ref-1 expression and activity in human prostate cancer cell lines and determine the effect of selective redox function inhibition on prostate cancer cells in vitro and in vivo. Since survivin expression is a known gene target of oncogenic transcriptional activators NFκB and STAT3, we additionally sought to assess APE1/Ref-1's redox function as a viable target to halt prostate cancer cell growth and survival. Our study demonstrates that survivin and APE1/Ref-1 are significantly higher in human prostate cancer specimens compared to noncancerous controls and that APE1/Ref-1 redox-specific inhibition with small molecule inhibitors APX3330 and APX3330 decreases prostate cancer cell proliferation and induces cell arrest. Additionally, NFκB transcriptional activity, survivin mRNA and survivin protein were significantly reduced upon redox inhibition of APE1/Ref-1. These data indicate that APE1/Ref-1 is a key regulator of survivin and a potentially viable target in prostate cancer.

## INTRODUCTION

Prostate cancer (PCa) is the most common male malignancy and the second leading cause of cancer-related death of men in the western hemisphere. [] Small prostatic carcinomas exist in up to 29% of men in their thirties and 64% of men in their sixties

with most of these carcinomas being indolent and curable by surgery or radiation. [] However, some men develop an aggressive phenotype that metastasizes and becomes incurable once colonizing the bone. [] These bone metastases produce osteoblastic lesions that are associated with high morbidity and high mortality [] and attempts at delaying this tumor progression with chemotherapeutic agents have only prolonged survival a few months. [] This necessitates a better understanding of the disease in order to create effective treatments for the aggressive phenotype where conventional therapeutics have failed.

Recently, it has been shown that reduction-oxidation (redox) regulation of critical transcriptional activators plays an essential role in cell proliferation and survival in a number of different cancers, including prostate cancer. Apurinic/apyrimidinic endonuclease 1 redox factor 1 (APE1/Ref-1) is a multifunctional protein that participates in DNA repair and redox transcriptional regulation. [] APE1/Ref-1 has been implicated in the development and progression of numerous cancer types along with being conversely correlated to tumor radiation and chemotherapy sensitivity. [] It is known to be overexpressed in prostate cancer. APE1/Ref-1 redox regulation of cysteine residues within the DNA binding domain or transactivation domain is essential for full transcriptional activation of certain transcriptional activators including the oncogenic transcriptional activators AP-1, HIF-1α, NF-κB and STAT3. Treatment with small molecule redox-specific inhibitors APX3330 and APX2009 have been shown to diminish the activity of these redox-regulated transcriptional activators. [] Furthermore, the blockade of APE1/Ref-1's redox activity has been shown to reduce growth-promoting, inflammatory and anti-apoptotic activities in cells. []

The ability of cancer cells to overcome apoptotic signals is crucial for tumor progression. Survivin, an Inhibitor of Apoptosis (IAP) family member, is overexpressed in prostate cancer and has been implicated in resistance to various chemotherapeutic and pro-apoptotic agents. [] Survivin is classically known as an inhibitor of caspases due to its single BIR domain, but recently survivin has been found to be crucial in cell cycle progression as a member of the chromosomal passenger complex. [] Our lab previously has shown that survivin is juxtaposed to inflammation in human prostate cancer specimens and may play a role in repair and recovery of prostatic tissue. [] Attempts at directly targeting survivin have ultimately failed in clinic, therefore a clinical need for new therapeutics blocking the expression of survivin persists.
Accumulating evidence demonstrates that APE1/Ref-1 is a key regulator of cancer cell growth and survival signaling. Here, we report that inhibition of APE1/Ref-1 redox activity decreases prostate cancer cell proliferation, transcriptional activity of NFκB, and downregulates survivin expression in prostate cancer cells in vitro and in vivo. This is the first report to our knowledge to show mechanistically that APE1/Ref-1 redox-specific inhibitors are a viable therapeutic option for prostate cancer treatment.

## RESULTS

### APE1/Ref-1 and Survivin are Overexpressed in Human Prostate Cancer

To confirm that APE1/Ref-1 and survivin expression is altered in prostate cancer, we performed immunofluorescence using human non-diseased and cancerous prostate specimens (Figure 1A). We found that APE1/Ref-1 is overexpressed in prostate cancer compared to non-diseased control prostates and it co-localizes with survivin-expressing

cells (71% co-localization in primary tumor specimens and over 99% in metastatic specimens). Expression of both proteins was primarily found to be nuclear and localized to in the epithelium. To determine if well-characterized prostatic cell lines displayed the same pattern, PC-3, C4-2, LNCaP and E7 cell lysates were collected and immunoblotting was performed evaluating APE1/Ref-1 and survivin protein levels (Figure 1B). APE1/Ref-1 and survivin were found to be significantly higher ($p<0.05$ , Analysis of Variance [ANOVA]) in the prostate cancer cell lines compared to the noncancerous cell line E7 consistent with that observed in the human specimens.

**APE1/Ref-1 Redox Inhibition Decreases Prostate Cancer Cell Proliferation**

To determine if inhibition of APE1/Ref-1's redox function affects cell proliferation, prostatic cell lines were treated with increasing concentrations of redox-specific inhibitors APX3330 and APX2009 for 5 days and cell number was measured via methylene blue assay (Figure 2A-D). RN7-58, an inactive analogue of APX3330, was used as a negative control. APX3330 and APX2009, inhibited cell proliferation in a concentration-dependent manner. Growth $IC_{25}$'s and $IC_{50}$'s were determined and arranged in Table 1. APX2009 was found to be 5-10 fold more efficacious than parent compound APX3330 in inhibiting cell proliferation, while the inactive analogue RN7-58 had no effect on cell growth in these assays.

**APE1/Ref-1 Redox-Specific Inhibitors Decrease Survivin Protein Levels**

Because survivin plays an important role in prostate cancer cell proliferation and survival and is known to be upregulated via known APE1/Ref-1-regulated transcription factors in other organ systems [], we tested the possibility that treatment with APE1/Ref-

1 redox specific inhibitors APX3330 and APX2009 might decrease survivin protein levels. Prostate cancer cells treated with respective growth inhibitory EC50 drug concentrations of APX3330 and APX2009 exhibited a significant decrease in survivin protein abundance within 48 hours compared to DMSO treated controls (Figure 3A-D). In contrast, prostate cancer cell total APE1/Ref-1 protein levels were not significantly altered with treatment.

**APX2009 Reduces Survivin mRNA Expression and Perturbs NFκB Activity**

Based on the observation that treatment with APX2009 was able to reduce survivin protein levels, we next sought to determine the mechanism by which APE1/Ref-1 regulates survivin expression, and ultimately, cell growth. C4-2 cells were treated with DMSO or APX2009 (14 μM) for 12 hours. RNA was collected and RT-qPCR was performed using a primer/probe set for survivin (BIRC5) and HPRT1 for the internal control gene (Figure 4A) using conditions suggested by the manufacturer. Survivin mRNA was significantly reduced upon treatment with the RQ value being <0.5. Because it has been shown in other cancers that survivin is a gene target of NFκB and that NFκB is regulated by APE1/Ref-1, we evaluated the ability of these two proteins to physically interact with each other and the cellular localization of both NFκB and APE1 upon treatment with APX2009. In Figure 4B, we demonstrate via co-immunoprecipitation that APE1/Ref-1 interacts with NFκB subunit p65 when using an APE1/Ref-1 antibody and in reverse experiments using a p65 antibody. In Figure 4C, p65 and APE1/Ref-1 were found to be co-localized in the nucleus but p65 nuclear localization was diminished upon treatment with APX2009 suggesting disturbed NFκB signaling. To determine if NFκB signaling is regulated by APE1/Ref-1 redox activity, we transfected C4-2 cells

with NFκB-driven luciferase constructs. Treatment of these cells with APX2009 results in a significant decrease, in both basal NFκB activity and TNFa-induced activity (Figure 4D).

**Treatment with APX2009 induces G1 Cell Arrest but not Cell Death**

To determine if treatment with APX2009 results in cell death, PC-3 and C4-2 cells were treated with either DMSO or APX2009 (9 μM and 14 μM, respectively) for 48 hrs (Figure 5A) and cell lysates were collected for immunoblotting (Figure 5B). After APX2009 treatment, both PC-3 and C4-2 cells displayed an altered, flattened cellular morphology. However, treatment with these compounds did not induce cell death as determined by both a lack of increased caspase 3 cleavage and a lack of increase in TUNEL labeling. Because no increase in apoptosis was detected and G2/M cell cycle proteins were decreased, cell cycle analysis was performed with Propidium Iodide (PI) staining. PC-3 and C4-2 cells were treated with APX2009 (9 μM and 14 μM, respectively) for 48 hrs and then stained with PI and analyzed by flow cytometry. We found that the percentage of cells in G1 significantly increased, $p<0.05$ via Student's t-test, from 58 to 68% and 63 to 74% in PC3 and C4-2 cells, respectively. These effects on the cell cycle progression are similar to other recent reports of APE1/Ref-1 redox inhibition in cancer. []

**APE1/Ref-1 Redox Inhibition Decreases Survivin Protein Levels and Cell Proliferation In Vivo**

Based on the in vitro data, we further measured the role of APE1/Ref-1 redox activity in cell proliferation and survivin protein levels in vivo using C4-2 subcutaneous xenografts. In those animals treated with APX3330 (25 mg/kg bid) for 5 days, survivin intensity via

immunofluorescence was found to be diminished (Figure 6A) and total survivin protein via immunoblotting was reduced by 40% (Figure 6B) when compared to control tumors. Furthermore, BrdU incorporation was significantly reduced, $p<0.05$ via Student's t-test, from 5.36% to 3.47% in the treatment group supporting the notion that APE1/Ref-1 redox activity is important for tumor cell proliferation (Figure 6C). These results indicate that APE1/Ref-1 redox inhibition maintains its effects in vivo.

## DISCUSSION

Despite recent advances in prostate cancer treatment, challenges in targeting key drivers of the aggressive phenotype remain. , challenges in targeting key drivers of the aggressive phenotype remain despite recent advances in prostate cancer treatment. Aberrant survival signaling leads to induction of survival proteins, most notably survivin, which leads to increased proliferation, survival and resistance to current therapeutics (Figure 7). [] In this study, we provide evidence that by targeting redox regulator APE1/Ref-1 with small molecule inhibitors we effectively suppress survivin protein levels and inhibit cell proliferation.

APE1/Ref-1 is a multifunctional enzyme that was primarily discovered as an enzyme in the base excision repair (BER) pathway but has emerged as a redox regulator of transcription factors in cancer. [] These transcription factors, AP-1, STAT3 and NFκB, have been shown to be important in the initiation and progression of prostate cancer. Utilizing this unique ability of APE1/Ref-1 to target multiple different pathways at once is an advantageous therapeutic strategy and further supports the case for APE1/Ref-1 as viable target in prostate cancer. Our results indicate that APE1/Ref-1 and survivin are overexpressed in primary and metastatic tumors which is in accordance with what

Kelley et al [] has shown previously. APE1/Ref-1 protein was found to be primarily nuclear but cytoplasmic staining was present in the tumors. Currently, the cellular localization of APE1/Ref-1 has not been fully characterized and more research is needed to determine what differential staining patterns mean to the severity of the disease. We also found that this expression pattern to be true in the prostatic cell lines. This supported the use of these cell lines in the in vitro studies.

Inhibition of APE1/Ref-1 redox function has been shown to decrease cell proliferation in other cancer cell lines which is consistent with what we found in prostate cancer. [] Small molecule inhibitors APX3330 and APX2009 of APE1/Ref-1 redox activity lead to decreased cell proliferation in a concentration-dependent manner and induced G1 cell cycle arrest. APE1/Ref-1 knockdown also inhibited cell proliferation and replicated what was shown with the inhibitors (Supplementary Figure 2). The apparent discrepancy between our study and those where cells are arrested in G2/M due to direct survivin inhibition may be due to the upregulation of CDKi's that prevent entry into S phase which have been previously observed with inhibition of APE1/Ref-1's redox function. [] Furthermore, treatment with APX3330 and APX2009 resulted in the decrease of survival proteins Bcl-2, Mcl-1 and survivin, where survivin was the most consistent among the cell lines (Supplementary Figure 1).

Survivin is known to be differentially regulated in various tissues and in response to external stimuli. [] It has been shown in the literature that survivin can be transcriptionally regulated by a number of transcription factors including Sp-1, STAT3 and NFκB. [] In this study, we provide evidence that survivin is being transcriptionally regulated by NFκB but recognize the fact that other transcription factors might be

playing a role. We show that survivin mRNA is significantly reduced, that p65 cellular localization is disrupted and that NFκB luciferase activity is decreased after treatment with APX2009. This is in accord with other publications showing that NFκB is regulated by APE1/Ref-1. [] Further research is needed to determine which specific transcription factor is primarily responsible for survivin transcription.

Prostatic tumor xenografts treated with APX3330 displayed decreased survivin protein levels via immunofluorescence and immunoblot and cell proliferation via BrdU staining. APX3330 was used for the in vivo experiments due to it's more characterized pharmacokinetic and pharmacodynamics properties. In the future, APX2009 will be used a single agent and in combination with other therapeutics in vivo to validate it's in vitro results. Together, these data demonstrates that APE1/Ref-1 redox inhibition in vivo is a viable option to decrease survivin protein levels and ultimately slow down prostatic tumor progression.

## MATERIALS AND METHODS

### Cell Lines

PC-3, LNCaP and C4-2 prostate cancer cell lines were purchased from and authenticated by the ATCC (Manassas, VA). E7 prostate epithelial cells were from Dr. David Jarrard, Department of Urology, University of Wisconsin Madison. All cell lines were maintained at 37ºC in 5% CO2 and grown in RPMI (Corning: Manassas, VA) with 5% Fetal Bovine Serum (HyClone: Logan, UT).

### Immunohistochemistry

Human prostate specimens or C4-2 xenograft tumors were fixed in 10% formalin, processed routinely, embedded in paraffin, and serially sectioned at 5 μm via microtome. Tissues were subjected to heat-induced antigen retrieval in 10 mM citrate buffer (citrate buffer stock solution of monohydrate-free acid citric acid, sodium citrate dehydrate, pH 6.0) for 10 minutes followed by 10 minute rest. Sections were blocked at room temperature with a bovine serum albumin (BSA)-Donkey serum mixture for 2 hours and incubated with primary antibody overnight at 4 ˚C. Primary antibodies and dilutions included rabbit survivin (1:100, Cell Signaling Technologies), mouse APE1/Ref-1 (1:200, Novus Biologicals), rabbit BrdU U (1:200, Cell Signaling Technologies), and mouse PanCK (1:200, Cell Signaling Technologies). Sections were washed with 1X PBS ( Phosphate-buffered saline)-Tween and incubated with IgG Alexa 488 and IgG Alexa 594-conjugated secondary antibody against rabbit or mouse for 1 hour at room temperature (1:200, Invitrogen), followed by 10 minutes incubation with Hoechst 33258 nuclear stain (1μg/ml). Tissues were washed with 1x PBS-Tween and water and then covered with an aqueous medium/glass coverslips. The sections were analyzed by immunofluorescence.

**Human Specimens**

Human prostate specimens were obtained with appropriate minimal risk institutional review board approval according to the approval and guidelines at Indiana University School of Medicine. Sections were cut from pre-existing paraffin-embedded human prostate tissues obtained as part of a prostatectomy or from prostate specimens removed collaterally from bladder cancer patients undergoing cystoprostatectomy as control human specimens. These controls were age-matched to the prostate cancer

specimens and were verified by record to be naïve for pretreatment with Bacillus Calmette-Guérin (BCG) because these patients had presented first with muscle invasive bladder cancer. The controls were verified by pathology to be void of prostate cancer.

All human specimens were stained with survivin and APE1/Ref-1 antibodies for immunofluorescence, as described above.

**Immunoblotting**

Prostate cells were homogenized in lysis buffer containing protease inhibitor (150 mM NaCl, 10 mM tris, 1 mM EDTA, 1 mM benzenesulfonyl fluoride, and 10 µg/ml each of aprotinin, bestatin, L-luecine, and pepstatin A) and 1% Triton X-100. Total protein concentration was determined by BCA (bicinchoninic acid) assay (Pierce, Rockford, IL). 10 µg/well of Protein were resolved by electrophoresis in 4-15% gradient polyacrylamide gels (Bio-Rad Laboratories). Proteins were transferred to polyvinylidene difluoride (PVDF) membranes, blocked for 24 hours [(10% Dry milk, 5% BSA, .05% $NaN_3$) in 1xPBS( 2.7 mM KCl, 1.5 mM $KH_2PO_4$, 136 mM NaCl, 8 mM $Na_2HPO_4$)-Tween 20] and incubated overnight with one of the following primary antibodies: mouse β-actin (1:2500, ThermoFisher Scientific), mouse APE1/Ref-1 (1:1000, Novus Biologicals), rabbit survivin (1:500, Cell Signaling Technologies), rabbit Bcl-2 (1:500, Cell Signaling Technologies), rabbit Mcl-1 (1:500, Cell Signaling Technologies), rabbit Cleaved Caspase 3 (1:250, Cell Signaling Technologies), rabbit Total Caspase 3 (1:1000, Cell Signaling Technologies), rabbit Cyclin B1 (1:500, Cell Signaling Technologies), Cdc2 (1:1000, Cell Signaling Technologies) and rabbit GAPDH (1:1000, Cell Signaling Technologies). After blots were washed 6 times with PBS-Tween, blots were incubated

with donkey antibody against rabbit or mouse immunoglobulin G conjugated to horseradish peroxidase for 1 hour (1:10,000 dilution, Pierce) in nonfat dry milk,1X PBS, and .05% Tween 20. Peroxidase activity was detected via Pico chemiluminescence reagent (Pierce). Photo images were analyzed by densitometry.

**Methylene Blue Assay (Cell Proliferation)**

Prostate cells were seeded 1,000-5000 per well (cell line/experiment-dependent) and treated with either APX3330, APX2009 or RN7-58 for 5 days. Media was then removed and cells were fixed with methanol for 10 minutes and stained with 100 μL's of 0.05% of methylene blue (LC16920-1 diluted in 1X PBS) for 1 hour. The cells were then washed 3X with water and allowed to air dry overnight. 100 μL's of 0.5N HCl was added to each well to dissolve the methylene blue stain and absorbance (@630) was measured via spectrophotometry. The percent viabilities, normalized to DMSO, were graphed and $IC_{50}$ concentrations determined.

**Reverse Transcription-PCR**

RNA isolation was performed using RNeasy Mini Kit (Qiagen). 10 nanograms of total RNA was reverse transcribed using Superscript III One-Step RT-PCR System (ThermoFisher Scientific). Real-time PCR was performed using the TaqMan Gene Expression Assay (BIRC5 (Hs04194392_s1) and HPRT1 (Hs02800695_m1), ThermoFisher Scientific) and Applied Biosystems 7500 Fast Real-Time PCR System.

**Co-Immunoprecipitation**

Samples were co-immunoprecipitated using the Pierce Co-IP kit (Thermo Scientific). Additionally, the cells were washed twice with 1X PBS and the proteins were cross-linked using DTBP (Thermo Scientific, 5 mm, for 30 min on ice). DTBP was quenched by washing with cold inactivation buffer (100 mm Tris-HCl, pH 8, 150 mm NaCl) and 1XPBS. Cells were then lysed and the lysates added to columns and after extensive washing, the bound proteins were eluted and prepared for immunoblot analysis.

**Luciferase Assay**

C4-2 cells were co-transfected with constructs containing luciferase driven by NFκB (pLuc-MCS with NFκB responsive promoter; PathDetect cis-Reporting Systems, Stratagene, La Jolla, Ca) and a Renilla luciferase control reporter vector pRL-TK (Promega Corp., Madison, WI) at a 20:1 ratio by using Effectene Transfection Reagent (Qiagen; Valencia, CA). After 16 hrs, cells were treated with increasing concentrations of APX2009 in serum free media for 24 hrs and then 10 ng/mL TNFα for 6 hrs. Firefly and Renilla luciferase activities were assessed by using the Dual Luciferase Reporter Assay System (Promega Corp.). Renilla luciferase activity was used for normalization and all transfection experiments were performed in triplicate and repeated 3 times in independent experiments.

**Propidium Iodide Cell Cycle Analysis**

PC-3 and C4-2 cells were treated with APX2009 (9 and 14 μM, respectively) for 48 hours. 500,000 cells were then aliquoted for cell cycle analysis and 0.1 mg/ml Propidium Iodide and 0.6% NP-40 PBS stain wash was added to the tubes. The cells were then centrifuged at 1900 rpms for 10 minutes with the brake on low and then

decanted and blotted. RNAase and stain wash were added and cells incubated on ice for 30 minutes. Propidium Iodide intensity was measured via flow cytometry.

### In Vivo Subcutaneous Tumor

$2 \times 10^6$ C4-2 cells were subcutaneously implanted in the hind flank of male athymic nude mice using a 100µl volume of 50:50 solution of Matrigel: RPMI medium. When tumor volumes reached150 -200 $mm^3$, the animals were treated every 12 hours with 25 mg/kg IP APX3330 for 5 days. BrdU was injected into the animals 2 hours prior to sacrifice and tumor tissues were analyzed for survivin levels (immunofluorescence and immunoblotting) and BrdU incorporation (immunofluorescence).

### siRNA Transfection

All siRNA transfections were performed using the HiPerfect Transfection Reagent (Qiagen) protocol. Samples for immunoblotting were collected 72 hours post transfection of cancer cells with APE1/Ref-1 siRNA and scrambled siRNA control. Prevalidated APE1/Ref-1 siRNA (siAPE1 #2) was purchased from LifeTech (#s1446).

## Statistics

Summary statistics are presented using the mean, median, and SD. Either a Student's t-test or ANOVA test was performed to compare the groups as appropriate. Statistical significance was assessed at the $p < 0.05$.

## Figures

**Figure 1** APE1/Ref-1 and survivin are overexpressed in human prostate cancer. A: (1,2) Hematoxylin and Eosin staining representing non-diseased (peripheral zone taken from cystoprostatectomy) and cancerous human prostate specimens. Scale bar = 100 μM. (1',2') Immunofluorescent images of stained non-diseased and cancerous sections for APE1/Ref-1 (red) and survivin (green). Scale bar = 50 μm. B: Representative pictures of prostate cancer cell lines (PC-3, C4-2 and LNCaP) and noncancerous prostate cell line (E7). Images were taken at 20x magnification with the scale bar = 50 μm C: Immunoblot example of basal survivin and APE1/Ref-1 protein levels between the prostatic cell lines. Representative of three determinations with densitometry quantification, N=3, *-denoting $p<0.05$ (PC-3, C4-2, LNCaP vs. E7) within ANOVA.

**Figure 2** APE1/Ref-1 redox function specific inhibitors decrease cell number in a concentration dependent manner. A-D: PC-3, C4-2, LNCaP and E7 cell lines were treated with increasing concentrations of redox-specific inhibitor APX3330, more potent analogue APX2009, and inactive analogue RN7-58 for 5 days (N=3). The cells were fixed and stained with methylene blue and measured via spectrophotometry. IC25 and IC50 were determined as the concentrations of drug at which there was a 25% and 50% reduction in absorbance compared to DMSO and were used for subsequent experiments.

**Figure 3** Treatment with APX3330 and APX2009 decreases survivin protein levels. PC-3, C4-2, LNCaP and E7 cell lines were treated with DMSO, IC25 and IC50 drug concentrations for 48 hrs. Immunoblotting for survivin, APE1/Ref-1 and Actin as labeled. Representative of three determinations with densitometry quantification, N =3, *-denoting $p<0.05$ (DMSO vs. IC25 and IC50 Drug Concentrations) within ANOVA.

**Figure 4** APE1/Ref-1 redox inhibition decreases survivin protein levels via NFκB. A: C4-2 cell line was treated with DMSO or APX2009 (14 μM) for 12 hours. RNA was isolated and RT-PCR for survivin was performed with HPRT1 as the internal control. B: C4-2 cell line was treated with DMSO or APX2009 for 48 Hrs and immunofluorescence was perfumed using antibodies for APE1/Ref-1 (Red) and NFκB subunit p65 (Green). Representative images were taken. Scale bar = 50 μM. C: Immunoblot validation of APE1/Ref-1 and p65 Co-Immunoprecipitation (Co-IP) reactions. The input and IP were loaded for each reaction. Mock beads and generic IgG were used as negative controls. D: C4-2 cells were transfected with NFκB–Luc construct and co-transfected with a Renilla vector, pRL-TK. After 16 hrs, cells were treated with increasing concentrations of APX2009 for 24 hrs, and Firefly and Renilla luciferase activities were assayed using Renilla luciferase activity for normalization. 10 ng/mL TNFα 6 hrs prior to lysis was used to induce NFκB activity. All transfection experiments were performed in triplicate and repeated 3 times in independent experiments. Data are expressed as Relative Luciferase Units (RLU) normalized to DMSO showing the mean ± SEM. N=3, *-denoting $p<0.05$ within ANOVA.

**Figure 5** APE1/Ref-1 redox inhibition induces G1 cell arrest. A: PC-3 and C4-2 cell lines were treated with DMSO or APX2009 (9 and 14 μM, respectively) for 48 hours. Representative images were taken at 20X Magnification. Scale bar = 50 μm. B: Immunoblotting was performed and membranes were probed with antibodies for Cleaved Caspase 3, Total Caspase, Cyclin B1, Cdc2, survivin and Actin as labeled. D: PC-3 and C4-2 cells were treated with DMSO or APX2009 (9 and 14 μM, respectively)

for 48 hrs and then collected and stained with RNAse/PI wash. Flow Cytometry was then performed. N =3, *-denoting $p<0.05$ within Student's t-Test

**Figure 6** In vivo treatment with APX3330 reduces survivin protein levels and BrdU incorporation in C4-2 xenograft tumors. C4-2 xenograft tumors were treated with vehicle (4% Cr: Et PBS) or APX3330 (25 mg/kg, IP bid) for 5 days (N=3). Tumors were removed and processed for either immunofluorescence or immunoblotting. A: Immunofluorescence was performed using APE1/Ref-1 (red) and survivin (green) specific antibodies on vehicle (1-4) and APX3330 (1'-4') groups. Representative images were taken. Scale bar = 50 µm. B: APE1/Ref-1 and survivin protein levels were measured using immunoblotting as labeled. C: Mice were injected with BrdU 2 hours prior to sacrifice and tumors were collected and stained for PanCk (red) and Brdu incorporation (green). Scale bar = 50 µm. ImageJ Nucleus Counter was used to quantify number of BrdU+ nuclei and total nuclei per image. N =3, *-denoting $p<0.05$ within Student's t-Test.

**Figure 7.** Model showing how cytokine/growth factor signaling induces survivin protein expression and at what points where APX2009/APX3330 disrupts this.

**Supplementary Fig. 1 A:** PC3, C4-2 and noncancerous E7 cells were treated with DMSO or redox-function inhibitors APX3330 and APX2009 and probed with antibodies for Bcl-2, Mcl-1, survivin, APE1/Ref-1, and Actin for immunoblotting as labeled.

**Supplementary Fig. 2 A:** PC-3 and C4-2 cell lines were transfected with 50 nM APE1/Ref-1 siRNA (verified >70% knockdown by immunoblotting) and growth was

compared to scrambled siRNA-transfected cells. B: Representative pictures of fixed and methylene blue stained C4-2/PC-3 scrambled siRNA (Scr), survivin siRNA #1 (siAPE1 #1) and #2 (siAPE1 #2). C: Immunoblotting was performed using antibodies for APE1/Ref-1, survivin and Actin as labeled. N =3, *-denoting $p<0.05$ within Paired Student's t-Test (Scr vs siAPE#1), #- denoting $p<0.05$ within Paired Student's t-Test (Scr vs siAPE#2).

**Table 1** Growth IC25 and IC50's were determined for each cell line using the 3 growth curves for APX2009 and E3330. Data is presented as mean ± s.e.m.

**Figure 1:**

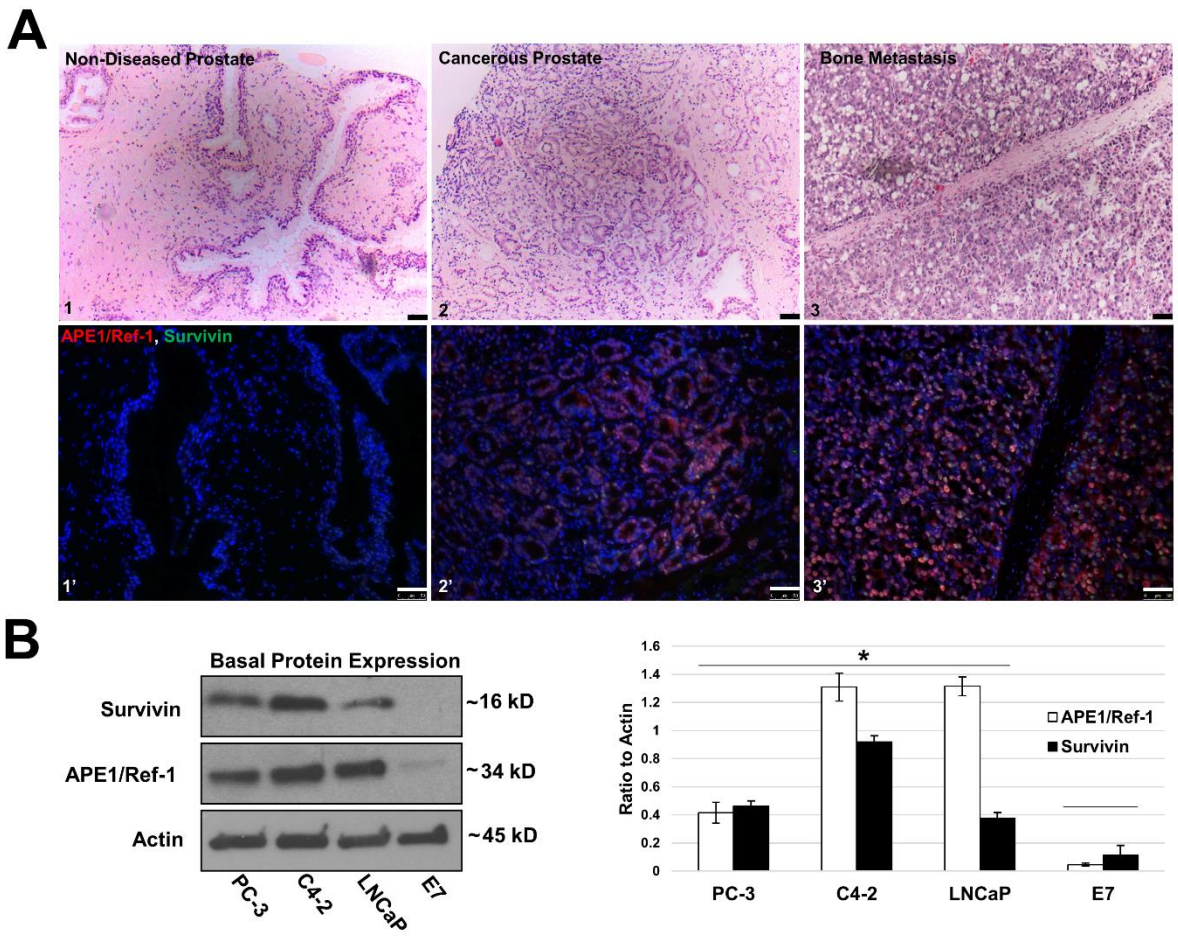
A
Non-Diseased Prostate
Cancerous Prostate
Bone Metastasis
1
2
3
APE1/Ref-1, Survivin
1'
2'
3'
B
Basal Protein Expression
Survivin
APE1/Ref-1
Actin
~16 kD
~34 kD
~45 kD
PC-3
C4-2
LNCaP
E7
Ratio to Actin
1.6
1.4
1.2
1
0.8
0.6
0.4
0.2
0
*
APE1/Ref-1
Survivin
PC-3
C4-2
LNCaP
E7

**Figure 2:**

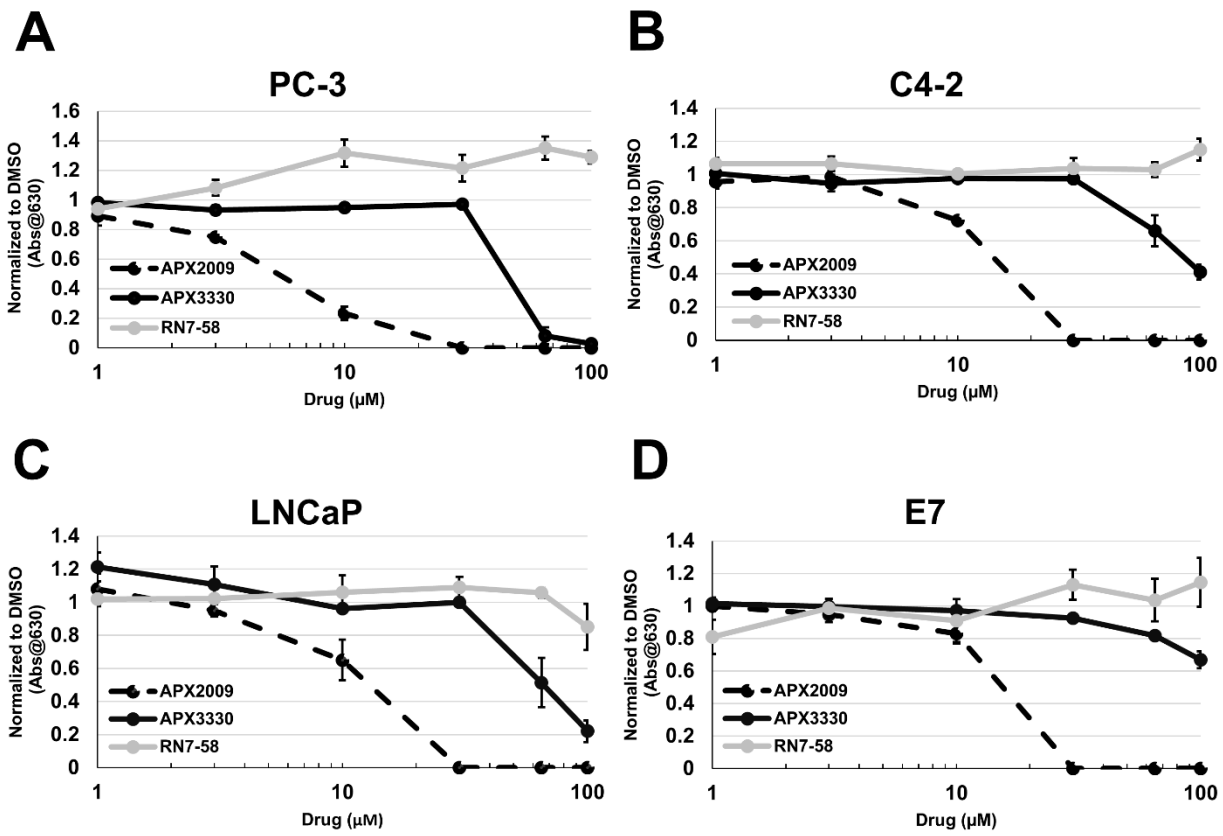
A
PC-3
B
C4-2
C
LNCaP
D
E7
Normalized to DMSO (Abs@630)
Drug (μM)
APX2009
APX3330
RN7-58

**Figure 3:**

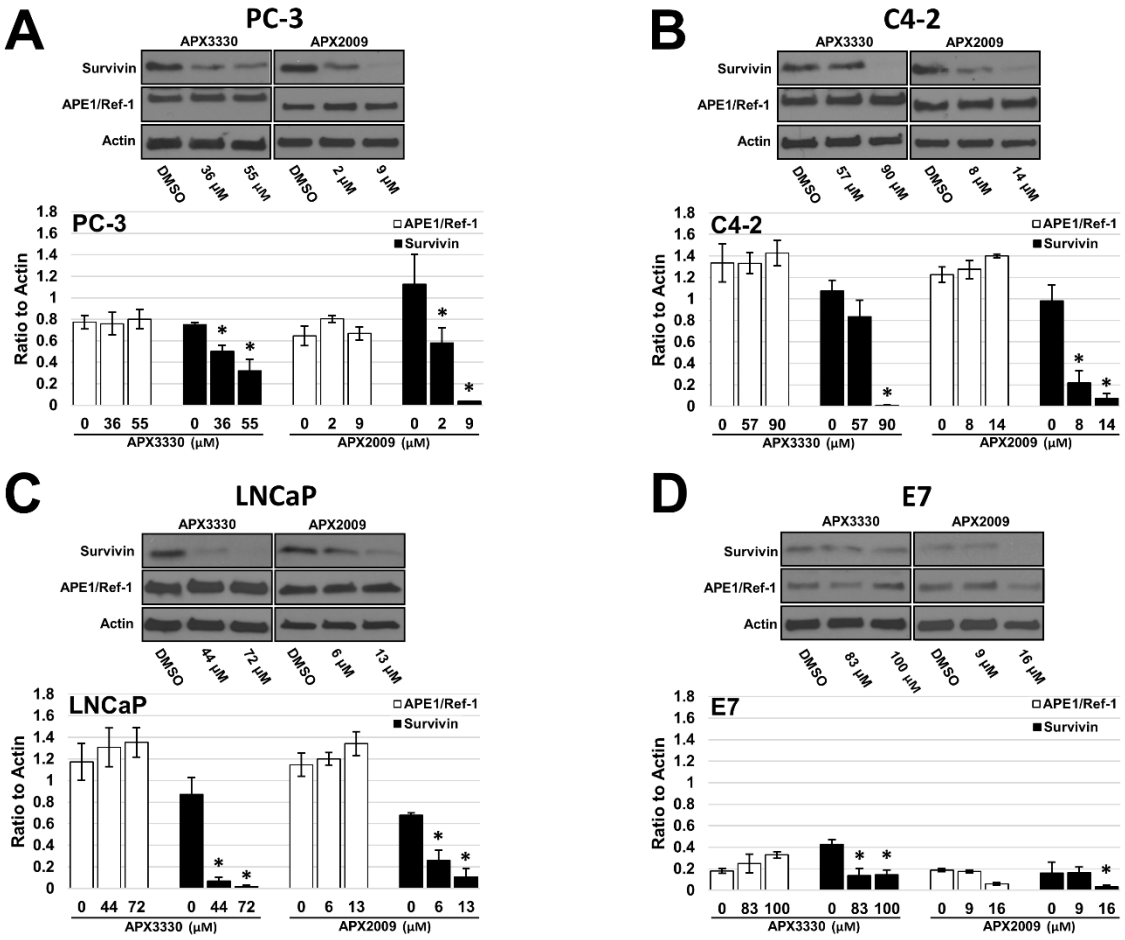
A
PC-3
APX3330
APX2009
Survivin
APE1/Ref-1
Actin
DMSO
36 μM
55 μM
DMSO
2 μM
9 μM
PC-3
□APE1/Ref-1
■Survivin
Ratio to Actin
0 36 55 0 36 55 0 2 9 0 2 9
APX3330 (μM)
APX2009 (μM)
B
C4-2
APX3330
APX2009
Survivin
APE1/Ref-1
Actin
DMSO
57 μM
90 μM
DMSO
8 μM
14 μM
C4-2
□APE1/Ref-1
■Survivin
Ratio to Actin
0 57 90 0 57 90 0 8 14 0 8 14
APX3330 (μM)
APX2009 (μM)
C
LNCaP
APX3330
APX2009
Survivin
APE1/Ref-1
Actin
DMSO
44 μM
72 μM
DMSO
6 μM
13 μM
LNCaP
□APE1/Ref-1
■Survivin
Ratio to Actin
0 44 72 0 44 72 0 6 13 0 6 13
APX3330 (μM)
APX2009 (μM)
D
E7
APX3330
APX2009
Survivin
APE1/Ref-1
Actin
DMSO
83 μM
100 μM
DMSO
9 μM
16 μM
E7
□APE1/Ref-1
■Survivin
Ratio to Actin
0 83 100 0 83 100 0 9 16 0 9 16
APX3330 (μM)
APX2009 (μM)

**Figure 4.**

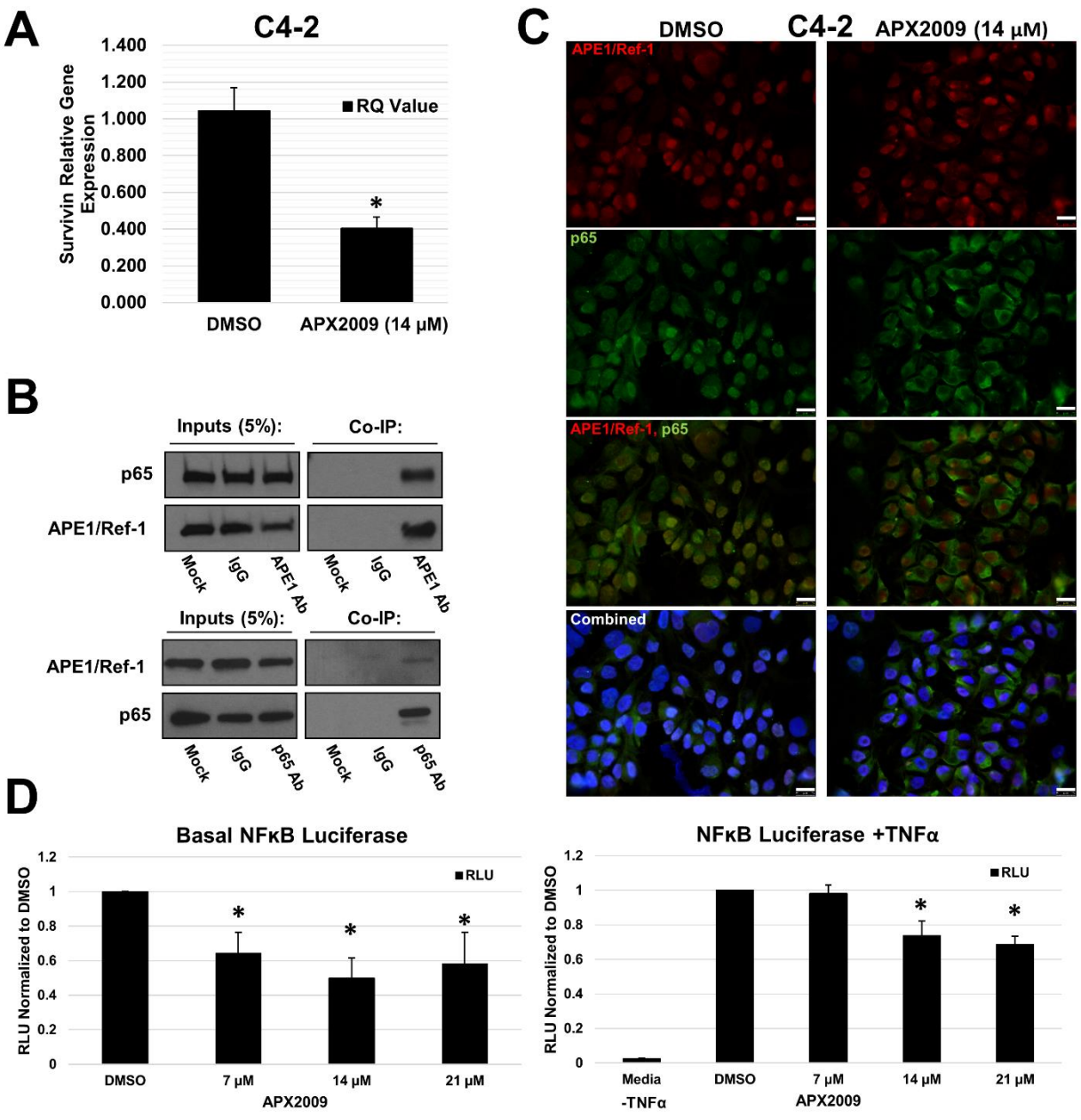
A
C4-2
Survivin Relative Gene Expression
1.400
1.200
1.000
0.800
0.600
0.400
0.200
0.000
RQ Value
*
DMSO
APX2009 (14 μM)
B
Inputs (5%):
Co-IP:
p65
APE1/Ref-1
Mock
IgG
APE1 Ab
Inputs (5%):
Co-IP:
APE1/Ref-1
p65
Mock
IgG
p65 Ab
C
DMSO
C4-2
APX2009 (14 μM)
APE1/Ref-1
p65
APE1/Ref-1, p65
Combined
D
Basal NFκB Luciferase
RLU Normalized to DMSO
RLU
DMSO
7 μM
14 μM
21 μM
APX2009
NFκB Luciferase +TNFα
Media -TNFα
DMSO
7 μM
14 μM
21 μM
APX2009

**Figure 5.**

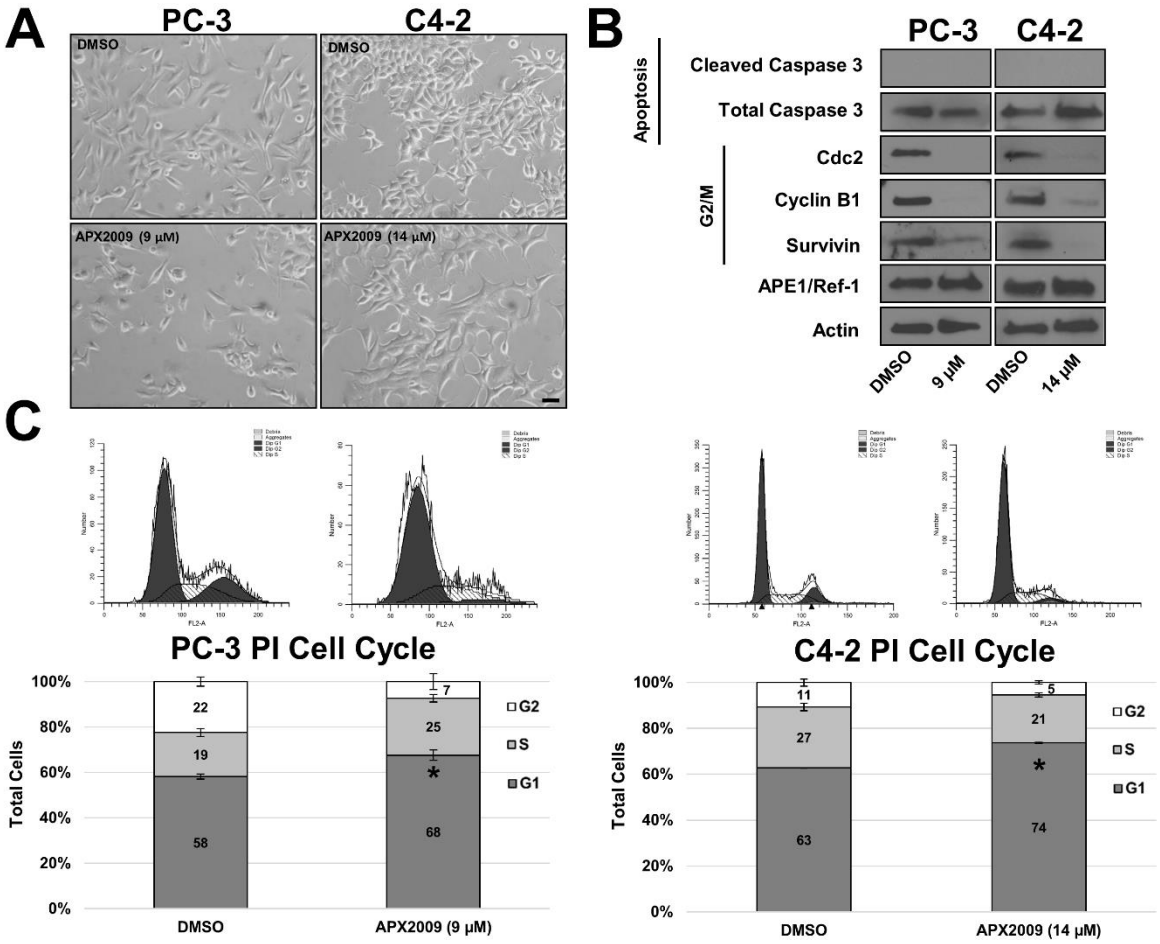
A
PC-3
C4-2
DMSO
DMSO
APX2009 (9 μM)
APX2009 (14 μM)
B
PC-3
C4-2
Apoptosis
Cleaved Caspase 3
Total Caspase 3
G2/M
Cdc2
Cyclin B1
Survivin
APE1/Ref-1
Actin
DMSO
9 μM
DMSO
14 μM
C
PC-3 PI Cell Cycle
Total Cells
100%
80%
60%
40%
20%
0%
22
19
58
7
25
68
*
G2
S
G1
DMSO
APX2009 (9 μM)
C4-2 PI Cell Cycle
Total Cells
11
27
63
5
21
74
*
G2
S
G1
DMSO
APX2009 (14 μM)

**Figure 6.**

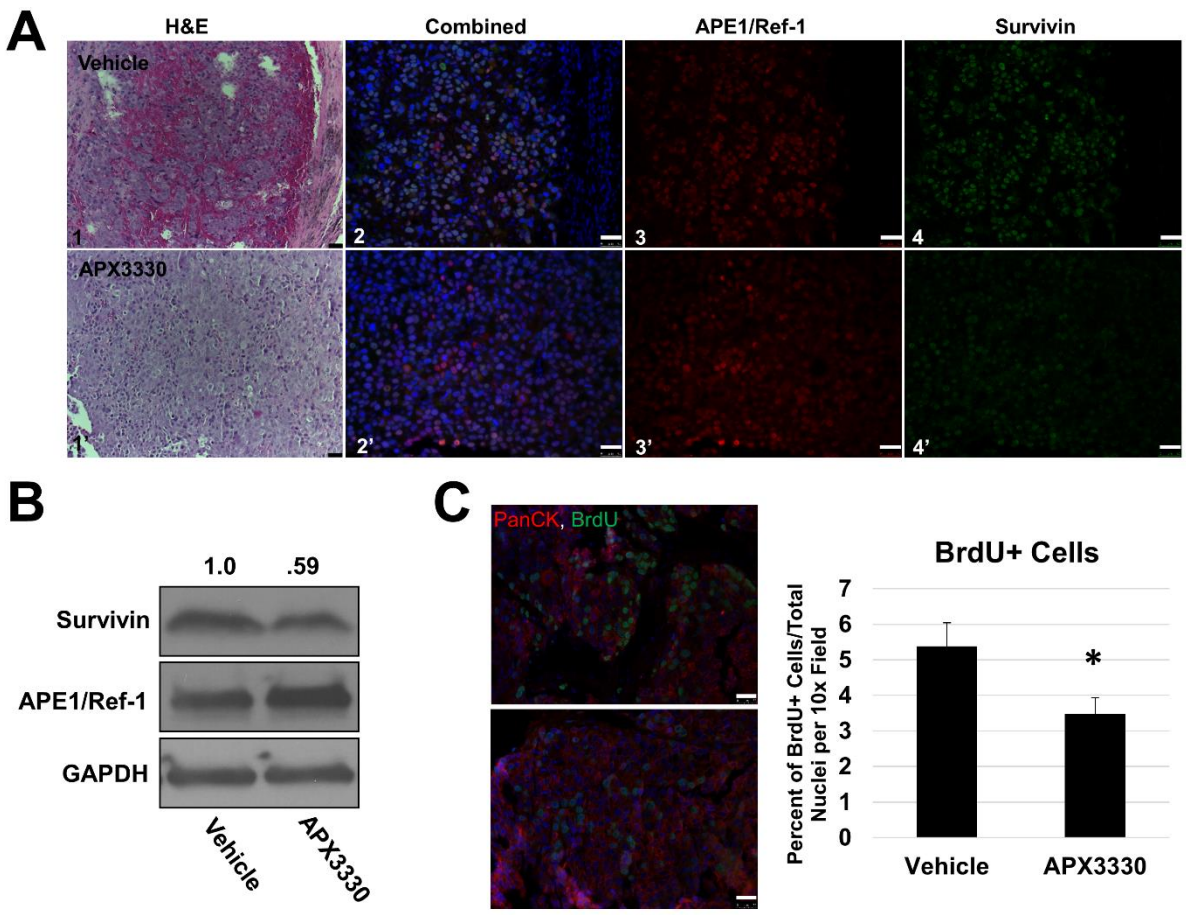
A
H&E
Combined
APE1/Ref-1
Survivin
Vehicle
APX3330
1
2
3
4
1'
2'
3'
4'
B
1.0
.59
Survivin
APE1/Ref-1
GAPDH
Vehicle
APX3330
C
PanCK, BrdU
BrdU+ Cells
Percent of BrdU+ Cells/Total Nuclei per 10x Field
0
1
2
3
4
5
6
7
*
Vehicle
APX3330

**Figure 7.**

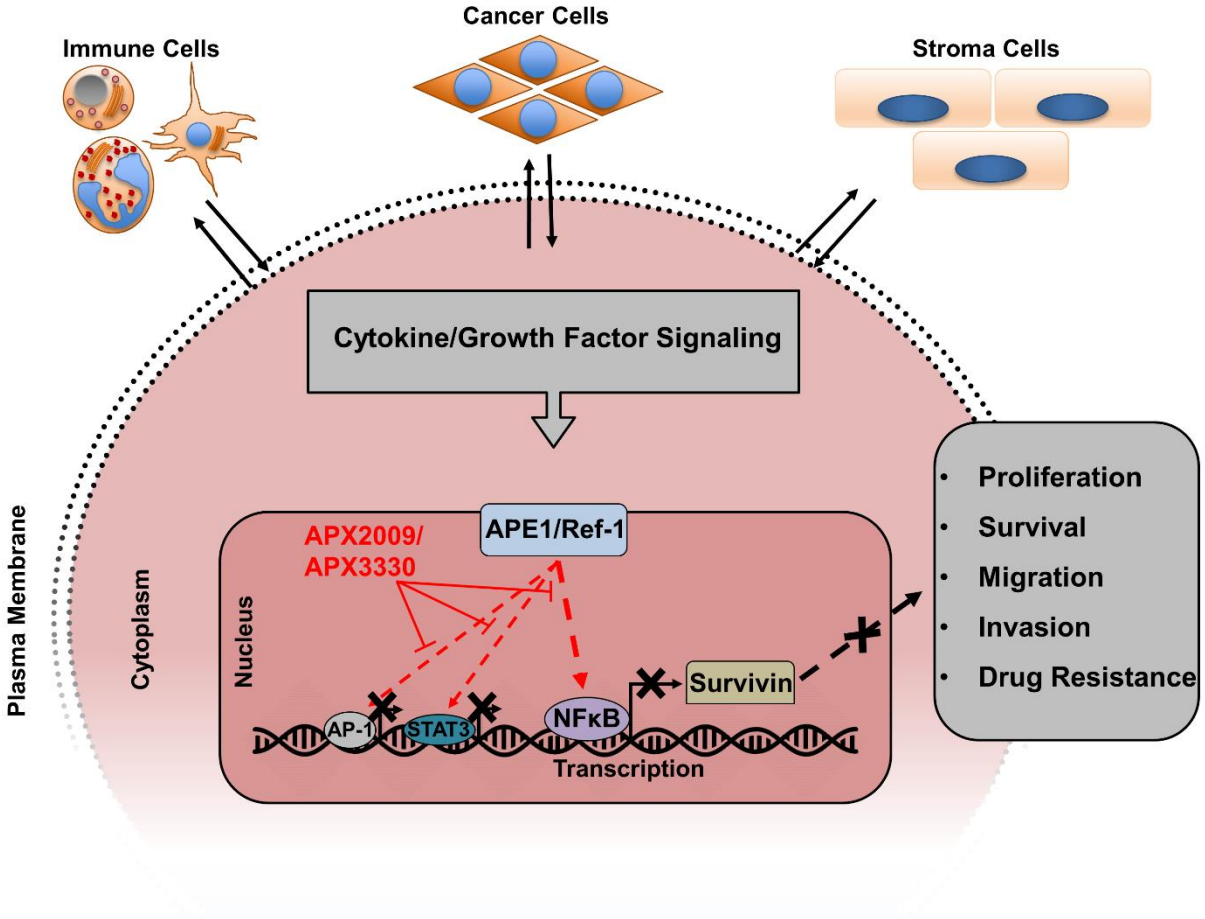
Cancer Cells
Immune Cells
Stroma Cells
Cytokine/Growth Factor Signaling
Plasma Membrane
Cytoplasm
Nucleus
APX2009/
APX3330
APE1/Ref-1
Survivin
AP-1
STAT3
NFκB
Transcription
Proliferation
Survival
Migration
Invasion
Drug Resistance

**Supplementary Figure 1.**

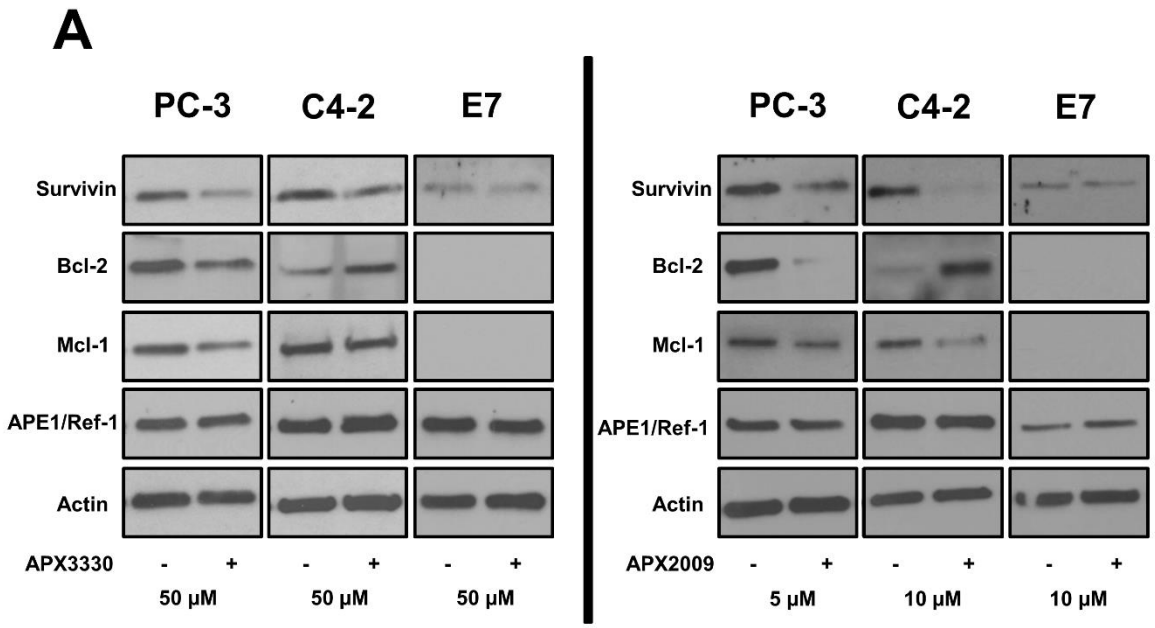

**Supplementary Figure 2.**

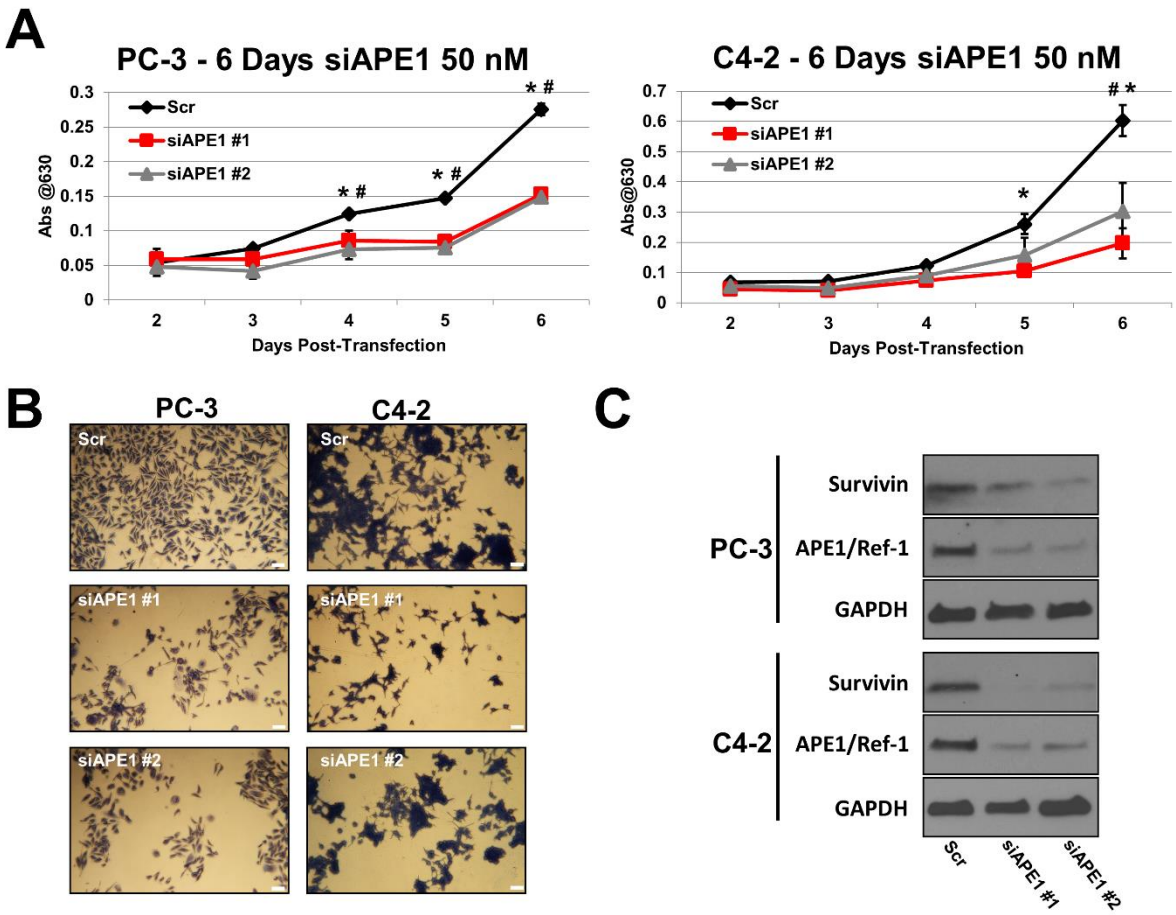

**Table 1.**

| | | E3330 | APX2009 |
|---|---|---|---|
| PC-3 | $IC_{25}$ | 36.0 +/- 1.0 | 2.2 +/- .5 |
| | $IC_{50}$ | 54.7 +/- 1.6 | 8.9 +/- .7 |
| C4-2 | $IC_{25}$ | 57.4 +/- 3.8 | 7.6 +/- .2 |
| | $IC_{50}$ | 89.5 +/- 7.8 | 14.2 +/- .3 |
| LNCaP | $IC_{25}$ | 43.8 +/- 4.2 | 6.3 +/- 1.6 |
| | $IC_{50}$ | 71.9 +/- 7.2 | 13 +/- 1.2 |
| E7 | $IC_{25}$ | 82.7 +/- 8.7 | 9.2 +/- .7 |
| | $IC_{50}$ | >100 | 16.1+/- .8 |